Paleogeographic and Sedimentary evolution of the South-Pyrenean Foreland basin.

Miguel Garcés[1], Miguel López-Blanco[1], Luis Valero[1,2], Elisabet Beamud [3,4], Josep Anton Muñoz[1], Belén Oliva-Urcia[5], Andreu Vinyoles[1], Pau Arbués[1], Patricia Cabello[1], Lluís Cabrera[1].

[1]Department of Earth and Ocean Dynamics & Geomodels Research Institute, Faculty of Earth Sciences, Universitat de Barcelona, Spain

[2]now at: Department of Earth Sciences, University of Geneva, Switzerland

[3]Institute of Earth Sciences Jaume Almera, CSIC, Barcelona, Spain

[4]Paleomagnetic Laboratory CCiTUB-ICTJA CSIC, Barcelona, Spain

[5] Dept. Geología y Geoquímica, Universidad Autónoma de Madrid, Spain

Abstract

During the Paleogene and Neogene the NE Iberian plate underwent significant paleogeographic changes driven by the Iberian and European plate collision and the resulting formation of the Pyrenean orogen and its corresponding foreland basin. Shortening resulted in the advance of the orogenic wedge, emplacement of allocthonous units, and progressive basin partitioning. Sediment transfer systems reacted to the evolving paleogeographic scenario, shifting from forebulge to foredeep and wedge-top settings. Critical reorganizations included successive shifts from open to close drainage conditions, which had an strong impact on accommodation, and the stratigraphic

architecture of the basin infill, overfill and later erosion. The aim of this work is to synthesize the paleogeographic and sedimentary evolution of the south-pyrenean foreland, with emphasis on the reconstruction of sediment routing, the evaluation of sedimentation rate trends, the timing of sedimentary shifts and the analysis of their causes. Stratigraphic data are compiled in a comprehensive magnetostratigraphy-based chronostratigraphic framework. Besides, sedimentary and structural data are put together to produce a series of palinspastically restored paleogeographic maps, which reflect five key stages in the evolution of the region. These stages include: 1) the Late Cretaceous tectonic inversion of the extended Iberian margin; 2) the Early Eocene formation of the southern Pyrenean foredeep; 3) the Middle Eocene widening and overfilling; 4) the late Eocene shift into an internal drainage; and 5) the Late Miocene drainage opening and erosion. In the light of these results, the variable role of tectonics, climate and eustacy at different time scales are discussed.

Contents

1. Introduction

Foreland systems are regions where a complex interplay between deep and surface processes is established (DeCelles, 2012; DeCelles and Giles, 1996; Sinclair, 1997), so that trigger and feedback relationships are not easily distinguished. Plate collision processes transform the landscape by means of high amplitude vertical movements of uplift and subsidence. Physical properties of the lithosphere determine the amplitude and wavelength of the flexure of the subducting plate, the first-order contributor of accommodation to the foreland basin. The evolution through geologic time, however, also depends on other factors such as climate and their feedbacks (Molnar and England, 1990), as surface processes of erosion and sediment transport are the agents of mass redistribution over the Earth surface and across the source-to-sink systems, from the internal to the external areas of the foreland system (Beaumont et al., 1992).

Understanding the causal relationships which operate in foreland systems relies on the analysis of the sedimentary record and its placement in a robust chronostratigraphic frame. Fine time lines are needed to link forcing mechanisms and their effects, to correlate disparate records and to frame the evolution of a study region in the overall evolution of the planet. In this paper, the long-term trends of sedimentation in the South-Pyrenean Foreland Basin (SPFB) (Fig. 1) are analyzed in the context of its paleogeographic evolution and the key times of basin configuration change. This is achieved thanks to the exceptional preservation of the stratigraphic record and abundant biostratigraphic and magnetostratigraphic studies carried out in the past decades, which allowed the construction of a reliable picture of the evolving sedimentary environments and routing systems through time. We review the evolution of the South-Pyrenean sediment transfer systems and sinks, from the Early Eocene chain-parallel turbiditic troughs to the late Eocene to Miocene internally drained Ebro basin, and the final fluvial incision and drainage opening towards de Mediterranean basin.

2. The setting of Pyrenean thrust-belt and its southern foreland basin

The Pyrenean orogen formed as a result of the north-directed convergence and continental collision between Iberia and European plates since the Late Cretaceous. Crustal-scale cross-sections based

on seismic data and abundant additional geophysical data show evidence that the Iberian lower crust has subducted or underthrusted together with the lithospheric mantle underneath the European plate (Chevrot et al., 2018; Muñoz, 1992; Teixell, 1998).

Continental collision led to tectonic inversion of pre-existing Mesozoic rifted margins during the Late Cretaceous (García-Senz, 2002), followed by the growth of the doubly-vergent orogenic wedge during the Paleogene. Flexural response of the lithosphere caused the formation of two peripheral basins, a pro-foreland basin on the subducting iberian plate, and a retro-foreland basin on the overriding european plate. Low-temperature geochronological data confirm geological constraints and mark the onset of continental collision at ca. 70Ma and acceleration and widening of the collision front at 50Ma (Fitzgerald et al., 1999; Mouthereau et al., 2014). Zircon fission-track ages show a distinctly diachronous growth of the Pyrenean orogen, characterized by a younging trend from north to south across the Axial Zone and from East to West (Whitchurch et al., 2011).

The southern Pyrenees are formed by a set of imbricate thrust sheets that developed in a piggy-back sequence from Late Cretaceous to Early Miocene (Cámara and Klimowitz, 1985; Choukroune, 1989; Muñoz, 1992; Muñoz et al., 2018b; Vergés, 1993; Vergés et al., 2002a), although some were reactivated by a break-back thrust sequence during the Uppermost Eocene-Lower Oligocene (Muñoz, 2002; Vergés and Muñoz, 1990). Triassic salts acted as the primary detachment level, to the extent that their occurrence along the northern Iberian margin determined the structural style and the location and geometry of allochtonous units. In the Eastern and Central Pyrenees the Mesozoic cover is detached along the Triassic salts from the Hercinian basement. Basement rocks form an antiformal stack of high tectonic relief in the Axial Zone, while the Mesozoic cover is involved into a series of thrust sheets grouped into three main units. In the central Pyrenees, these are The Bóixols-Cotiella, the Montsec-Peña Montañesa and the Gavarnie-Serres Marginals thrust sheets (Fig. 1). In the eastern Pyrenees these are the Upper Pedraforca, the Lower Pedraforca and the Cadí-Montgrí thrust-sheets. In the western Pyrenees, the absence of Triassic salts favored a deformation style in the form of a wider and lower relief imbricated system where sedimentary cover and basement are coupled (Teixell, 1996).

Restored cross-sections across the Pyrenees show minimum total shortening of about 110-125km in the Eastern Pyrenees (Grool et al., 2018; Vergés, 1993) and 150km at the Central Pyrenees (Muñoz, 1992). Mountain building caused the flexure of the Iberian plate and the development of an E-W elongated deep foreland basin draining towards the Atlantic Ocean (Puigdefàbregas, 1975; Séguret, 1972). The forward migration of the orogenic wedge onto the subducting plate caused progressive basin partitioning, and foredeep sedimentation being gradually shifted into a wedge-top setting. The emplacement of the Montsec thrust sheet in the Paleocene-Early Eocene resulted in the early piggy-back transport of the Tremp-Graus basin. The Tremp-Graus basin has a simple internal structure of an E-W elongated gentle syncline bounded in its southern margin by the Montsec thrust and to the north by the Bóixols thrust and southward tilted beds above basement-involved thrust sheets.

The emplacement of the Cadí and the Gavarnie-Serres Marginals thrust sheets during the Middle Eocene resulted in the piggy-back transport of a wider foreland region, which included the Ripoll basin in the eastern Pyrenees (Vergés et al., 1995), the Ainsa basin and, finally the Jaca basin in the western Pyrenees (Labaume and Teixell, 2018; Muñoz et al., 2013, 2018b). The deformation along the frontal thrust of the Southern Pyrenees continued until the Early Miocene, and involved progressively younger detachments in the Paleogene sedimentary fill, at the level of the Beuda evaporites (Early-Middle Eocene) and the Late Eocene salts and evaporites of the Cardona and Barbastro formations (García-Senz and Zamorano, 1992; Vergés et al., 1992).

The current basement geometry under the SPFB consists of an asymmetric double flexure caused by the main load of the Pyrenean wedge and, secondarily, the tectonic load of the Iberian and Catalan Coastal Ranges (CCR). The westward narrowing of the foreland basin, bounded by the Sierra de Cantabria and the Cameros-Demanda massifs (Fig. 1), caused superimposed flexure from both margins, and maximum basement deepening under the La Rioja trough (Muñoz-Jiménez and Casas-Sainz, 1997), reaching depths of as much as 5000mbsl (Pardo et al., 2004), compared to 3800mbsl in the Eastern Pyrenean margin. In the undeformed areas of the eastern SPFB, beyond the influence of the Pyrenean load, the basement is found at 900mbsl south of Lleida. There, subsidence is mainly driven by the sediment load that accumulated well above sea level since the closure of the basin drainage. Shallow depths of the basement in the easternmost regions of the

SPFB are caused by the overprint of the Neogene to Pleistocene rifting and shoulder uplift of the NE Iberian plate (Vergés and Fernández, 2006).

3. Chronostratigraphic framework

The main stratigraphic units of the SPFB and their vertical and lateral relationships are synthesized in two chronostratigraphic charts, along a North-South transect from Eastern Pyrenees to Catalan Coastal Ranges (Fig. 2) and an East-West transect along the Tremp-Graus, Ainsa and Jaca basins (Fig. 3). The most outstanding feature in the eastern N-S transect (Fig. 2) is the general southward displacement of facies belts and basin depocenters (Puigdefàbregas et al., 1986). Non-marine alluvial sediments (Mediona, Pontils) are overlain by shallow marine platforms (Cadí, Orpí, Peña, Tavertet, etc) and later by deep marine foredeep successions (Sagnari, Armàncies, Banyoles, Igualada) in an overall transgressive trend onto the southern margin. This, together with the stratigraphic onlap onto the passive margin observable from subsurface data in central sectors (ITGE, 1990; Vergés et al., 1998) was the result of the advance of the deformation front driven by plate convergence and underthrusting of the Iberian plate.

In the E-W transect across the Tremp-Graus, Ainsa and Jaca basins (Fig. 3), the most outstanding feature is the westward deepening of sedimentary environments, from proximal alluvial to fluvial in the Tremp-Graus basin, to slope and deep marine in the Ainsa and Jaca basins, and the abyssal plains of the peripheral oceanic basin of the Bay of Biscay. Added to this, facies belts are organized in a transgressive-regressive sequence from Paleocene to late Eocene. The lower transgressive trend represents the southwards migration of the plate flexure, with shallow carbonate platforms (Guara, Boltaña, etc.) being replaced by foredeep environments (Hecho Group). This is then followed by a progressive filling of the foredeep and westwards progradation of the axially fed fluvio-deltaic system (Capella, Escanilla, Campodarbe). The transition from marine to continental sedimentation yields a same age in both the east and western sectors of the SPFB, indicating that basin continentalization did not represent the reaching of an overfilling stage, but the result of the closure of the external drainage (Costa et al., 2010).

Three main erosional episodes leading to regional unconformities are represented in Figure 3. The first developed in the Jaca basin between the Paloecene carbonate platforms and their overlying

deep marine deposits of the Hecho Group. The corresponding hiatus could result from a combination of processes such as forebulge development, starvation following drowning of the platforms, and instabilization and collapse of the out-of-grade platform margins (Payros et al., 1999b; Vinyoles et al., 2019). The second erosional episode developed in the Tremp-Graus basin during the Lutetian. It was caused by the wedge-top uplift associated to the southward transport of the Gavarnie thrust-sheet and the emplacement of deep-seated thrust sheets involving basement. The third erosional episode relates to a broader uplift phase that involved the Tremp-Graus and Ainsa basins during the Eocene-Oligocene transition. This was followed by continued aggradation of alluvial sediments that buried the orogenic wedge in a context of endorheic basin configuration.

The present study relies on a chronostratigraphic framework built upon an integrated marine and continental biostratigraphy and magnetostratigraphy. Larger foraminifera biostratigraphic data is available from the abundant shallow marine environments of the southern margin carbonate platform units (Guara, Boltaña Fm., etc.), and mixed platforms interbedded within deltaic sequences (Sobrarbe Fm., Tossa Fm.). Larger foraminifera are also abundant as reworked elements in mass-transport deposits filling the slopes and turbiditic troughs of the Ripoll, Ainsa and Jaca basins. The development of a Shallow Benthic Zonation provided among the first chronostratigraphic framework of the SPFB, which ranged from Paleocene to late Priabonian age (Serra-Kiel et al., 2003a, 1994; Serra−Kiel et al., 1998). Biostratigraphic data from planktonic foraminifera is abundant in the open and deep marine sediments of the Jaca-Pamplona basin (Alegret et al., 2009; Canudo et al., 1988; Molina et al., 2011; Payros et al., 1999a), and scarce in the more restricted and shallower marine environments that characterized the eastern regions of the Pyrenean foreland, which often yield poorer microfossil assemblages (Cascella and Dinarès-Turell, 2009; Caus, 1973; Ferrer, 1971; Hottinger, 1960). Mammal vertebrate findings of chronostratigraphic interest are scarce in the Early to Middle Eocene but crucial to coarsely constrain the age of alluvial and fluvial sediments filling the La Pobla de Segur, Tremp-Graus and Ripoll basins (Badiola et al., 2009; Bonilla-Salomón et al., 2016). Vertebrate fossil findings were more abundant from late Eocene to Middle Miocene (Agustí et al., 2011; Cuenca Bescós et al., 1992; Murelaga et al., 2008, 2004), as the marine gateway closure of the SPFB triggered extension of terrestrial environments to the whole basin.

Magnetostratigraphic data from the SPFB spans its complete stratigraphic record from Paleocene to middle Miocene, and includes representative sections from all sub-basins and basin margins (see references in caption of Fig. 4). These have allowed to build a robust chronostratigraphic framework that integrates the varied sources of biostratigraphic information (Fig. 4). Robustness of this chronostratigraphic framework does not rely on a number of fixed geochronologic or biochronologic tie points which tightly anchor the correlation scheme. Instead, magnetostratigraphic correlation relies on the match with the Geomagnetic Polarity Time Scale (GPTS) (Ogg et al., 2016) that best agrees with all external (biostratigraphic and/or radiometric) age constrains. Because true uncertainties associated to both biostratigraphic and radiometric ages often fall within the 100kyr to one-million-year range, the final correlation is ultimately guided by the best fit between the local magnetostratigraphy and the GPTS. In doing this we rely on the observation that long-term (>100kyr) sedimentation unsteadiness do rarely come close to the intrinsically aperiodic and highly variable duration of geomagnetic polarity chrons (Fig. 5), and therefore a good match with the GPTS confidently indicates a correct magnetostratigraphic correlation. A magnetostratigraphic correlation independent of external age constraints is feasible as long as the local magnetic polarity sequence reveals a lengthy and characteristic pattern of magnetozones. Magnetostratigraphic sections spanning >15 well-defined polarity reversals, and on average >8 sites/magnetozone are favorable to yield a unique correlation with the time scale (Johnson and McGee, 1983). In practice, this is a fully achievable goal when the magnetostratigraphic work is planned at basin-scale.

The compilation of earlier magnetostratigraphic studies has allowed a robust correlation with the GPTS, and a further refinement of chronostratigraphic relationships of the main lithostratigraphic formations along the SPFB (Figs. 2 and 3). Selected magnetostratigraphic records were used to compile Age/depth plots in order to show the evolution of sedimentation rate trends of the different regions, from eastern to western Pyrenees, and from eastern to central areas of the Ebro basin (Figs. 6 to 10).

4. Evolutionary stages

Earlier synthesis on the tectonosedimentary evolution of the SPFB are focused on either the eastern Pyrenees (Barnolas, 1992; Burbank et al., 1992; Puigdefàbregas et al., 1986; Vergés et al., 2002, 1998), the central-western Pyrenees (Labaume et al., 2016; Muñoz et al., 2013; Nijman, 1998; Payros et al., 2009), or the younger stage represented by the Ebro basin (Muñoz-Jiménez and Casas-Sainz, 1997; Pardo et al., 2004). Here we aim at integrating the sedimentary and paleogeographic evolution of the overall SPFB as derived from its sedimentary record. To do so, marked changes in stacking patterns, sedimentary environments, sedimentation rates and depozone's localizations were considered to define five stages of basin-wide stratigraphic architecture,reorganization: 1) The Late Cretaceous-Paleocene tectonic inversion of the Mesozoic extensional basins; 2) The Early-Middle Eocene foredeep formation and fill; 3) The Bartonian basin widening; 4) The Late Eocene-Miocene internally drained basin; and 5) The Middle-Late Miocene basin opening. The interplay between tectonics and surface processes in the Pyrenean foreland system derived in a complex paleogeographic evolution, which is here illustrated in a series of paleogeographic maps (Fig. 11), each one depicting an evolutionary stage. In order to restore environments to their original relative positions, we included shortening values determined from balanced cross-sections from earlier studies (see references in caption of Fig. 11). Maps are constructed by considering displacement of thrust sheets relative to a fixed Iberian basement in its current coordinates.

Tectonic inversion of the Mesozoic rift basins (late Santonian-Paleocene)

The growth of the Pyrenean orogen started in the Late Cretaceous (late Santonian) with the inversion of pre-existing extensional faults, forming the Upper Pedraforca thrust sheet in the eastern Pyrenees and the Bóixols-Cotiella thrust sheet in the Central Pyrenees (Muñoz et al., 2018a). The shallow marine strait that connected the Tethys and Atlantic oceans progressively narrowed leading to the emersion of the eastern Pyrenean region (Plaziat, 1981). Sedimentation in the Paleocene of the central and eastern Pyrenees was characterized by the red mudstone "Garumnian facies" of the Tremp Group (Fig. 3), interbedded with lacustrine units. These continental sediments graded westward into marine carbonate platforms of the central-western Pyrenees and to deep marine sediments in the Basque Pyrenees (Fig. 11A). Alluvial systems were sourced from low relief emerged areas of the Iberian margin as well as from the rising northeastern

Pyrenees (Pedraforca, Bóixols, Montsec and Biure thrust sheets). The stratigraphic thickness of the Paleocene averages some 200m meters and represent a period of relative quiescence with low sediment input. However, greater thicknesses up to 700 m of Paleocene sediments accumulated along the axis of the Tremp-Graus syncline (Cuevas, 1992) on top of the Montsec thrust sheet, and as much as 900 m on top of the Lower Pedraforca thrust sheet (ITGE, 1990) thus indicating syn-kynematic sedimentation.

The Paleocene-Eocene transition was marked by a widespread Ilerdian transgression (Ferrer, 1971) that resulted in the expansion of shallow carbonate platforms (Alveolina limestone) along the Iberian margin and that extended southwards to areas now forming part of the Catalan Coastal Ranges (Anadón et al., 1979a) (Fig. 2). It correlates with a marked period of flooding of continental areas worldwide, and a gradual rise of sea level which peaked at 100 masl, the highest global sea level of the Cenozoic era (Miller et al., 2005a).

Despite the relative quiescence of the Paleocene period, fanning of beds on the southern margin of the Tremp-Graus and the northern margin of Àger basin already indicates the syntectonic character of sedimentation. The Montsec, however did not act as a persistent topographic barrier to sediment fluxes, as indicated by the reconstructions of the Early Eocene fluvial network connecting the Ager and the Tremp-Graus basins (Nijman, 1998). Sediment accommodation was maintained positive as to keep almost buried the rising Montsec at this early stage, the local uplift above the Montsec footwall ramp being compensated by the regional subsidence of the bending Iberian plate.

Formation of the South-Pyrenean foredeep (Early-Middle Eocene).

The Early Eocene was the period of most intense continental plate collision, with total shortening rates of up to 6 mm/yr (Vergés et al., 2002). This period correlates with the activity of the Lower Pedraforca, Montsec-Peña Montañesa , Lakora, Eaux Chaudes-Larra and Monte Perdido thrusts system in the Eastern, Central and Western Pyrenees respectively (Labaume and Teixell, 2018; Muñoz et al., 2018a). The uneven distribution of the Triassic evaporites caused the formation of a thrust salient in the central Pyrenees (Séguret, 1972) which resulted into the partitioning of the south Pyrenean sediment transfer system. Sediments sourced from the Eastern Pyrenees did no longer flow into the Tremp-Graus basin. At this time the Ripoll basin turned into a rapidly

subsiding sediment sink, while a connection with the Atlantic Ocean along a shallow marine passage to the south of the South-Pyrenean Central Unit (SPCU) was maintained. This scenario of basin compartmentalization that prevented longitudinal flow from the Eastern Pyrenees to the Tremp-Graus basin has been challenged by other researchers (Thomson et al., 2017), on the basis of an eastern Pyrenean source for pre-Hercinian zircons found in sediments from the Tremp-Graus and Ainsa basins. But, similar population of zircons are found in sediments of La Pobla de Segur basin, which only implies that the catchment areas of the Tremp-Graus fluvial system extended well into the Axial Zone (Michael et al., 2014). Our reconstructed map for the early Lutetian allows for a sediment routing system connecting the catchment regions in the eastern Pyrenees with the Tremp-Graus and Ainsa basins, to the north of the Ripoll basin (Fig. 11B).

Magnetostratigraphic ages of the >5000m thick Ripoll basin infill (Burbank et al., 1992; Vergés et al., 1998), are here revised to reconcile with the extended occurrence of SBZ13 benthic foraminifera at the Armàncies, Campdevànol and topmost marine Coubet formations (Busquets et al., 1992; Ramos et al., 2002; Tosquella and Samsó, 1996), and the updated calibration of this biozone in the SPFB (Molina et al., 2011; Rodríguez-Pintó et al., 2012). We are aware that the proposed correlation conflicts with the Bartonian age attributed to the overlying Bellmunt conglomerate Fm., on the basis of its vertebrate fossil assemblages (Bonilla-Salomón et al., 2016; Busquets et al., 1992). Further studies on the calibration of Eocene vertebrate faunas are needed to solve this and other issues related to the Eocene mammal biochronology (Beamud et al., 2003b).

Derived sedimentary trends in the Ripoll basin (Fig. 6) show steady low rates during the Paleocene, followed by a sharp increase to rates of 90 cm/kyr at 50Ma. This increase correlates with a rapid basin deepening represented by the transition from the fluvial/littoral facies of the Corones Fm. to the slope marls and turbiditic facies of the Armancies and Campdevanol formations. It was interpreted as the result of the southwards migration of the flexural subsidence caused by the tectonic loading of the Pedraforca and Montgrí thrust sheets along the northern margin of the basin (Puigdefàbregas et al., 1986). The turbiditic trough was fed with sediments sourced from the northern margin and rapidly filled with an east-to-west sense of progradation. This was coeval with thick evaporitic plugs (Serrat, Beuda and Besalú formations) and carbonate platforms (Penya and Tavertet formations) backstepping towards the southern margin (Fig. 2). The lateral continuity

of the carbonate platforms along the Iberian margin evidences that a seaway to the Atlantic Ocean remained open during this time and until the late Eocene. The marine passage was as shallow as to restrict water exchange with ocean waters, favoring precipitation of thick evaporite units, stratification of water column.. Anoxic bottom favoring preservation, high sedimentation rates, and rapid burial of organic matter were conditions met in the Ripoll basin during deposition of the marls and carbonatic turbidites of the Armancies Fm, thus enhancing preservation of their organic carbon of marine origin. Sediments of Armancies Fm. can be qualified as typlical oil shales, having high TOC values, which can reach individual scores of about 14% (Permanyer and Valles, 1988). Maturity parameters are typical of initial oil window, highlighting its potential as hydrocarbon source rock worth targeted during oil exploration in the Eastern Pyrenees (Caja et al., 2006; Kendall et al., 2019; Permanyer and Valles, 1988). The overlying siliciclastic turbidites of the Vallfogona Fm contain a fair content of organic carbon (1%), with a significant contribution from terrestrial plants, and a maturity stage at the very beginning of the oil window. The total estimated volume of hydrocarbon in the Vallfogona Fm. alone, however, does not represent a source of economic potential (Caja and Permanyer, 2008). It must be noted that hydrocarbon generative sedimentary units formed in the early stages of foreland evolution, and their preservation during the later stages of orogenic wedge exhumation were limited (Kendall et al., 2019).

It is remarkable that overfilling of the Ripoll foredeep was rapidly reached in only 5Myr, with the alluvial sediments of the Bellmunt Formation prograding across the basin by the latest Cuisian-early Lutetian, while subsidence was kept at very high rates. Altogether suggest that the Eastern Pyrenean Foreland underwent an effective sedimentary trap during the Early Eocene. The emplacement of the Montsec and the Lower Pedraforca thrust sheets, coupled with flow and accumulation of Triassic salt to the south of the Montsec as a consequence of its tectonic emplacement of the thrust sheet and sediment load in the area (Santolaria et al., 2016; Soto et al., 2002), prior to the emplacement of the Sierras Marginales thrust sheet, possibly acted to sustain a topographic barrier for sediments sourced from the Eastern Pyrenees, promoting fast accumulation and filling of the Ripoll basin.

Towards the western edge of the Montsec, the Ainsa Oblique Zone formed as a result of development of thrusts and related folds coeval to vertical axis clockwise rotation (Muñoz et al.,

2013). Accumulated rotations up to 70º resulted from differential thrust displacement between the Central and Western Pyrenees from early Lutetian to Oligocene as a result of the distribution of the Triassic evaporites. The transition from the Tremp-Graus basin, in the hangingwall of the Montsec thrust, to the Ainsa basin, in its footwall, is marked by a sudden change in the sedimentary environment, thickness and bathymetry. The fluvial and coastal marine sediments filling the Tremp-Graus basin grade laterally into slope and deep marine thick sedimentary sequences of the Ainsa and Jaca basins.

Sedimentary trends in the Jaca basin were constructed by compiling earlier stratigraphic (Barnolas and Gil-Pena, 2002; Payros et al., 1999a) and magnetostratigraphic studies (Hogan and Burbank, 1996; Oms et al., 2003). Along the northern flank of the Guarga syncline a preserved thickness of more than 6.000 meters spans from Paleocene to late Eocene (Fig. 7). A sharp transition from foreland carbonate platform to deep turbiditic trough took place at circa 50 Ma, and correlates with the emplacement of the Lakhora- Eaux-Chaudes thrust (Labaume et al., 2016; Labaume and Teixell, 2018). This is the same age of basin deepening as recorded in the Ripoll basin, and therefore points to a parallel acceleration of tectonic loading and foreland basin flexure from East to West. But, in contrast to the Ripoll basin, the increase of sedimentation rates in the Jaca basin shows a progressive trend, from very low sedimentation rates in the Paleocene and Early Eocene to average and steady rates of 65 cm/kyr of the Middle Eocene. This is interpreted as a result of the different paleogeographic and sediment routing system configuration. At the time of sedimentation of the Hecho Group the northern margin of the Jaca basin was either not emerged, or of very low-relief (Fig. 11B). Therefore, sediments were sourced from the East, from catchment areas located in the central and eastern Pyrenees (Michael et al., 2014), and then routed along a lengthy longitudinal transfer system. The coarser fraction of the sediment volume was trapped upstream, in the fluvial to shallow marine environments of the La Pobla de Segur, Tremp-Graus and Ainsa basins, while sedimentation in the Jaca-Pamplona basin was dominated by pelagic mudstones and sheet-like lobe and basin plain sandstone turbidites (Mutti, 1984; Remacha and Fernández, 2003). The western connection with the ocean allowed a portion of the finest fraction bypassing towards the abyssal plains of the Gulf of Biscay, that underwent the final sink of both the southern and northern Pyrenean foreland basins (Payros et al., 2006; Pujalte et al., 2002).

In spite of the fact that the Early Eocene was a time of intense deformation in the SPFB, the imprint of climate forcing in the stratigraphic architecture of the deep slope to basin floor distal siliciclastic systems has been investigated. In the Ainsa (Cantalejo and Pickering, 2014; Pickering and Bayliss, 2009; Scotchman et al., 2015) and the Jaca-Pamplona basins (Payros and Martínez-Braceras, 2014) turbiditic sequences were claimed to correlate with orbital eccentricity cycles. These were interpreted as supply-driven sequences of 10^5kyr, which were able to propagate along the full length of sediment transport system. Alternatively, and using stable-isotope proxy records, a link with sea level fluctuations was proposed, as much of the deep-water sediment gravity flow deposits in the Ainsa basin appear to be emplaced during eustatic lowstands (Castelltort et al., 2017).

Basin widening and overfilling (late Middle Eocene).

At the transition from Lutetian to Bartonian a remarkable shift in the facies belts is recorded in the South-Pyrenean foreland basin (Fig. 11C). Along the axis of the Jaca basin a shift from deep turbiditic systems (Hecho Group) to deltaic sediments (Larrés and Pamplona prodelta marls, Sabiñánigo and Belsué-Atarés deltaic sandstone) (Fig. 3) witnesses the progressive filling of the trough (Payros et al., 1999a). This was coeval upstream with the progradation of the fluvial (Escanilla Fm.) over the deltaic and slope (Sobrarbe and San Vicente Fms.) sediments in the Ainsa basin. Towards the southern margin (External Sierras), the Lutetian/Bartonian boundary is recorded with sharp vertical transition from platform carbonates (Guara Fm.) to siliciclastic sedimentation (Arguis and Belsué formations). This was preceded by a gradual increase of average sedimentation rates from 8cm/kyr to 23cm/kyr, rates that were maintained during the deposition of the uppermost Guara, Arguís and Belsué formations (Fig. 8). Towards the south-eastern basin margin, the Lutetian/Bartonian transition is marked by a transgressive sandstone unit (Seva, Folgueroles, Collbas Fms) which sharply overlies alluvial continental sediments of the Pontils and Romagats formations, and is followed by deposition of deeper marine marls of the Igualada Fm, (Fig. 9). This overall transgressive trend over the SPFB southern margin has been interpreted in the frame of the long-term southwards transport and growth of the pro-wedge, causing an acceleration and southwards migration of the subsidence through time (Puigdefàbregas et al., 1986), and the onset of structuration and tectonic loading along the CCR (Gómez-Paccard et al., 2012; López-Blanco, 2002). Added to this, a punctuated influence of climate and high-frequency

sea-level fluctuations was put forward to explain the nearly synchronous decline of carbonate platforms over the Iberian margin (Huyghe et al., 2012). During the Bartonian and Priabonian, some carbonate platforms persisted in the southern basin margin, but these were of limited extent and duration. Transient sea level and temperature oscillations and changes in rainfall patterns related to climate perturbations near the Lutetian-Bartonian transition, such as the Late Lutetian Thermal Maximum (Westerhold et al., 2018) and Middle Eocene Climatic Optimum (MECO) (Methner et al., 2016; Mulch et al., 2015; Rego et al., 2018), could have contributed to the rapid sedimentary shifts observed at this time. Transgressive-regressive sequences are found to occur in-phase with 400kyr eccentricity cycles in the Sant Llorenç del Munt and Montserrat fan-delta complexes (Gómez-Paccard et al., 2012) and the Belsué deltaic system in the Sierras Exteriores (Kodama et al., 2010), providing support for the occurrence of glacioeustatic driven sequences in the greenhouse world of the Late Eocene (Miller et al., 2005).

In addition, the late Middle Eocene was characterized by the progressive backfilling and burial of paleoreliefs with alluvial conglomerates, as observed at the Sierra de Sis and La Pobla de Segur basin of the Central Pyrenees (Coney et al., 1996). This, together with the transient development of lacustrine environments in the Tremp-Graus basin (Escanilla limestone), La Pobla de Segur (Ermita Fm) and Cajigar (Cornudella Fm) points to a period of increasing accommodation, an unexpected situation for units being deposited in a wedge-top setting. It is worth noting that the load associated to the growth of the antiformal stack in the Axial Zone certainly contributed to generate accommodation, preferentially localized towards the northern margin.

The combined sedimentary trends observed in the different regions of the South-Pyrenean foreland indicate that the late Middle Eocene was a period of distributed accommodation, with transgressive units expanding towards the foreland, north-derived clastic systems prograding into the central parts of the basin and proximal alluvial conglomerates onlapping paleoreliefs towards the hinterland. Tectonic load was distributed over larger areas due to the continued emplacement of the south-Pyrenean thrust units and, secondarily, the contribution from the CCR basement-involved thrust sheets (Gómez-Paccard et al., 2012; López-Blanco, 2002). This, combined with a punctuated period of high sea level could have favored the expansion of sedimentation areas, as

seen in other regions of the European plate (=Biarritzian transgression in Paris basin) (Borne et al., 1991).

The shift into an internally drained basin (Late Eocene).

Continuing growth of the Pyrenean thrust wedge, combined with the relief created by the bounding intraplate fold and thrust belts of the Iberian and Catalan Coastal ranges, led to a prolonged land-locked configuration (Fig. 11D) which persisted for approximately 25Myr. The shift into an internally drained basin, here known as the Ebro basin, was dated to 36Ma (Costa et al., 2010). Its sedimentary record is represented by a short-lasting isochronous deposition of marine evaporites and salts, enclosing two potash depocenters in the East (Catalan potash basin) and West (Navarra potash basin). The retreat of marine waters caused a transient drop of the base level, and accelerated progradation of siliciclastic systems of the Belsue-Atarés Fm (Fig. 3). Related to the basin desiccation event, localized erosion along the margins has been reported (Barnolas et al., 1981), but this situation was rapidly followed by a basinwide agraddational stacking of continental sediments. Magnetostratigraphic studies in different sections in the Jaca (Fig. 8) and the Ebro (Fig. 9) basins constrained the marine-continental transition to within a single chron (C16n.2n) (Costa et al., 2010), thus supporting the basinwide isochrony as well as the lack of significant erosional events related to basin desiccation.

The basin closure event represents the end of sediment bypass from the Jaca-Pamplona basin towards the Atlantic Ocean. An internally drained configuration allowed for a rising of the base level in phase with increasing sediment accumulation. This is graphically exemplified in the sedimentation trends across the marine-continental transition in the Jaca basin (Fig. 8), where a rapid and very significant increase of sedimentation rates coincides with the time of basin continentalization (Costa et al., 2010). Besides, in the Eastern Ebro this same transition also correlates with a sudden but transient increase of sedimentation rates, followed by a gradual return to trends of the previous externally drained stage (Fig. 9). This transient increase observed in the Igualada area (Fig. 9) could be a local response to the basinwards shift of accommodation just after diseccation. In the long-term trend we interpret that steady rates reflect a scenario where sedimentary systems fed from the Eastern Pyrenees and the CCR had their own sink in a shallow embayment of the eastern Ebro basin (Fig. 11C), bounded to the northwest by the Serres

Marginals-Sierras Exteriores thrust sheets. As a result, disconnection from the ocean sea had no or little effect in terms of sediment trapping.

Large endorheic regions are rare on Earth as surface erosion and sediment transport agents work together to keep the river draining network connected to sea level. The transition from open to closed drainage in the Ebro basin required a context where tectonic uplift rates in the western Pyrenees surpassed erosional processes, so that an emerged ridge formed a water divide between the south Pyrenean Foreland and its peripheral oceanic basin. It is plausible that the exact timing of closure was in concurrence with a sea level minima of the Late Eocene dated at approximately 36Ma (Van Sickel et al., 2004).

A continuous rise in the internal Ebro basin base level resulted from continuous sedimentary aggradation, leading to backfilling and burial of the surrounding reliefs of the Pyrenees (Coney et al., 1996) and CCR (Lawton et al., 1999) with alluvial conglomerates of late Oligocene age. Accumulated total thicknesses in central basinal domains ranged from 5km in the West (La Rioja) (Muñoz-Jiménez and Casas-Sainz, 1997) to 1km close to the southeastern margin of the Ebro basin (Jones et al., 2004).

Mixed alluvial-lacustrine sedimentation continued in the central and western Ebro basin until the late Middle Miocene. As a result, the Ebro basin evolved into an elevated (700-1000m above sea level) and low-relief plateau. Such an exceptionally long period of endorheism was favored by the relatively dry climate conditions, a key factor to both the formation of an internal drainage and its long-lived persistence (Garcia-Castellanos, 2007). It has been found that times of expansion of lacustrine environments were repeated cyclically at periods which correspond to Milankovitch frequencies, thus supporting orbital forcing. Times of high lake levels are correlated to maxima of the short (100kyr), long (400kyr) and very long (2.4My) orbital eccentricity (Valero et al., 2014). Among the recurrent periods of lacustrine spread and retreat, it is most remarkable the rapid development from 16.0 to 14.5 Ma of a vast fresh-water lake in the central areas of the Ebro basin (Alcubierre Fm) (Arenas and Pardo, 1999; Pérez-Rivarés et al., 2004, 2002) (Fig. 10), that replaced the evaporitic environments of the Early Miocene. The top of the evaporites of the Zaragoza Fm is truncated in the Sierra de Alcubierre by a 300kyr hiatus, which is the expression of the maximum retreat of the central lake. Transient times of dry climate and lowering lake levels, could lead to

localized sediment starvation in distal areas or even temporary exposition to erosion. The Middle Miocene Alcubierre limestone Fm. represents a rapid shift towards wetter conditions, in close correspondence with the global warming of the Middle Miocene Climatic Optimum (Zachos et al., 2001). Lacustrine environments persisted, at least, until the latest Middle Miocene (11.5Ma) as evidenced in the southwestern margin of the Ebro basin (Pérez-Rivarés et al., 2018). Evidences of endorheic sedimentation of Late Miocene or younger age are not preserved in the sedimentary record of the Ebro basin. In the surrounding and interconnected Duero, Almazán, and Calatayud basins (Figure 1), slow sediment aggradation continued into the late Miocene (9Ma, late Vallesian), giving rise to a flat-top basin infill of palustrine limestones. Connection between the Ebro and the Duero basins was at times feasible across La Bureba corridor (Salazar, 2003). Flexural isostasy corrections for erosional rebound of the deeply eroded Ebro basin indicate a paleoelevation of 530-700masl of the central Ebro basin at the end of its filling stage (Garcia-Castellanos and Larrasoaña, 2015).

Basin opening to western Mediterranean basin and erosion (late Miocene).

In the latest Oligocene a new geodynamic scenario is configured with the southeastwards drift of the Corso-Sardinian block, linked to back-arc extension and opening of the western Mediterranean basin. Rifting in the northeastern Iberian plate caused a high topographic gradient across its margin, driving accelerated erosion and fluvial incision (Fig. 11E). The composition of alluvial fan conglomerates filling the Valles-Penedès half-graben indicate that regions of the eastern Ebro basin were being captured by the upstream incision of a juvenile Llobregat river as early as early Tortonian (Garcés et al., 1996). But, among the rivers that incised across the horst-and-graben reliefs of the CCR, the Ebro river underwent the main route for sediments eroded from the Ebro basin and its bounding ranges. The chronology of the fluvial capture has raised some debate, with two competing visions. Some argue that the Ebro river could not exist earlier than the Messinian Salinity Crisis (MSC) because other Mediterranean rivers responded to the sea level drop following the MSC with a landwards deep canyon incision, and such a feature is not found along the Ebro river valley (Babault et al., 2006). Others, however, claim that a comparison of the juvenile Ebro river with other mature rivers such as the Rhone and the Nile is inappropriate, because these old rivers had a developed fluvial network better suited to react to substantial sea-

level drops and to carve out deep incised valleys (Arche et al., 2010). The absence of a Messinian canyon that propagated landwards for hundreds of km could be partially explained by later uplift experienced in the eastern Ebro basin and CCR due to rifting and erosional denudation (Juez-Larré and Andriessen, 2002; Lewis et al., 2000; Roca et al., 1999). The canyon, if existed, would have been uplifted and reshaped by later erosion. Numerical flexural modeling estimates an isostatic rebound of as much as 400m in the region where the Ebro river cross-cuts the CCR only due to erosional unloading (Garcia-Castellanos and Larrasoaña, 2015). Besides, a Messinian erosional surface of fluvial origin, incised offshore of the present Ebro river delta, was imaged by 3D seismic profiles, and interpreted to correspond to a river with a drainage area comparable to the present one (Urgeles et al., 2011), then supporting a pre-Messinian age for the capture of the Ebro basin.

Solutions taken from independent sources such as process-based modeling (García-Castellanos et al., 2003), thermochronology (Fillon et al., 2013), and magnetostratigraphic dating of the youngest endorheic sediments in the Ebro basin (Pérez-Rivarés et al., 2018), point to an age ranging from 11 to 9Ma for the opening of the Ebro basin. The onset of erosion of the Ebro basin would be related with the beginning of the deposition of the Castellón Group in the Valencia Trough, the oldest siliciclastic wedge of the Ebro delta, with a late Serravallian to Tortonian age (Arche et al., 2010; Evans and Arche, 2008). This scenario would be in agreement with the conclusions of a study of old terraces of the lower Ebro, of presumed late Miocene age, which contain clasts of Pyrenean source (Arasa-Tuliesa and Cabrera, 2018).

The estimated paleoelevation of the Ebro basin at the end of its filling stage was significantly lower than the base level of the surrounding Calatayud, Almazán and Duero basins, which were filled with sediments up to an approximate age of 9Ma (late Vallesian). These top sediments have not been intensively eroded, and they currently form a landscape of plateaus at an altitude of 1000masl. Cessation of lacustrine sedimentation in these basins was linked with a shift towards exorheic conditions, and a plausible scenario is that it was related to the upstream fluvial incision of the Ebro and its tributary Jalon river (Figs. 1 and 11E) (Salazar, 2003). We note that the process of capture of the Ebro basin internal drainage did not need to be a short catastrophic event. While the drainage divide was located along the axis of the CCR, the base level of the central lake could be found hundreds of km further west, where the locus of the subsidence during the Miocene was

located. Westward thicknening of Miocene sedimentary units indicates greater subsidence rates towards the La Rioja-Tudela area (Fig. 10). Meanwhile, the eastern Ebro basin experienced a decrease of accommodation space. Shoulder uplift associated to the rifting of the Iberian margin lead to a low relief westward tilted landscape over the CCR and eastern Ebro basin margin. Under these conditions, upstream erosion and fluvial capture of the internal drainage could be a long-elapsed process starting as early as Early Miocene and culminating with the capture of the central lake base level in the late Tortonian (9Ma, late Vallesian). Upstream fluvial incision is currently active in the la Bureba corridor, where the Ebro river is piracing the Duero basin headwaters (Pineda, 1996; Struth et al., 2019).

5. Tectonic and climatic driven sedimentary trends.

The long-term sediment accumulation in the SPFB was ultimately determined by tectonic-driven accommodation changes, of various sources which interfered through time and space:

1. Flexural response to tectonic loading of the Pyrenean orogen and, secondarily, the Iberian Range and CCR caused an asymmetric doubly-wedged sedimentary prism. Maximum sedimentary thicknesses of >7000m were allocated along the Pyrenean foredeep during the Early to Middle Eocene. Towards the eastern Ebro basin margin, in the area of Montserrat (Gómez-Paccard et al., 2012), tectonic load of the CCR allowed for flexural subsidence and accommodation of up to 2000m of sediments during the Middle to Late Eocene, before shifting to internally drained basin. Further southwest along the basin margin, in the area of Gandesa, the flexure associated to the load of the CCR was minimal, as subsidence was widely distributed due to the thin-skinned tectonic style of deformation. There, the sedimentary pile does not exceed in total 1000m (Jones et al., 2004), but the most of it were accumulated after closure of the basin drainage, when other factors rather than subsidence provided with accommodation space.
2. Tectonic closure of the marine gateway in the late Eocene, and the shift of the SPFB into an internally drained basin provided with additional accommodation, as the internal base level was allowed to rise pacing sediment aggradation. The SPFB turned into an efficient sediment trap, allowing expansion of the sedimentary environments beyond the flexural

wave to the limits of the land-locked depression. Towards the hinterland, sediments backfilled paleocanyons (Burbank and Vergés, 2004; Lawton et al., 1999; Vincent, 2001) and, eventually, buried the orogenic wedge (Coney et al., 1996). Stabilization of the frontal thrust wedge and reduction of the surface taper angle could have triggered tectonic growth in the orogen interior by underplating, and rapid antiformal stack exhumation. This scenario is coincident with the available chronology, as closing of the basin at 36 Ma (Costa et al., 2010) predates the phase of rapid exhumation of the Axial zone, dated to 32Ma (Fitzgerald et al., 1999).

3. Shoulder uplift of the eastern Iberian margin, due to the rifting of the Valencia trough (latest Oligocene-Miocene) contributed to an early diminishing of accommodation, to the point that no sediment accumulation occurred in the eastern Ebro basin possibly since the latest Oligocene. The landscape of eastern Ebro basin seemed like a low-gradient slope draining towards the western Ebro basin, where subsidence continued, and the Miocene units attain their greatest thicknesses (Fig. 11E).

A tectonic control on sediment accumulation was also exerted by way of crucial changes in the paleogeography, altering the sediment routing systems and the location of sinks. The submarine emplacement of the Montsec thrust sheet during lower Eocene and the related migration of the Triassic evaporites and mudstones towards the edges of the South Pyrenean Central thrust salient was key to isolate the Ripoll basin from the central South Pyrenean foredeep, and prevented from the westward sediment transport towards the abyssal plains of the Gulf of Biscay. The Ripoll basin turned into a sediment sink in front of the rising eastern Pyrenees, where maximum sedimentation rates of the overall SPFB infill, of nearly 1m/kyr, occurred during the early Eocene, leading to its rapid overfill. No evidence exists of sediments transferred from the eastern Ebro basin towards the Jaca-Pamplona basin, as the sallow sea connecting both regions southwards of the south-Pyrenean thrust front was permanently occupied by carbonate platforms.

Myr-scale climatic and eustatic oscillations were claimed to exert second-order control on the paleogeographic and sedimentary evolution of the SPFB and the precise timing of some key events. Warm temperatures and highstand sea-levels during the Early Eocene (Miller et al., 2005a; Zachos et al., 2008) favored the widespread distribution of marine environments and carbonate

platforms over the south-Pyrenean realm. Similarly, the later decline of carbonate platforms and their substitution by siliciclastic environments at the end of the Lutetian has been partially related to climate and sea-level fluctuations associated to the MECO. Higher frequency lower amplitude sea level changes appeared to play a role in stratigraphic architecture of both shallow and deep marine siliciclastic systems. Some of these records were suggested to pace with Milankovitch orbital frequencies, specifically with the 400kyr long eccentricity cycle (Gómez-Paccard et al., 2012). But untangling the nature of the forcing mechanism, related to either sediment supply (upstream) or base-level changes (downstream), is a challenge for future research in source-to-sink studies (Allen, 2017; Castelltort and Van Den Driessche, 2003; Romans et al., 2016; van den Berg van Saparoea et al., 2008).

After the shift into internal drainage, basin depocenters were occupied by a central lake. Sedimentary facies assemblages indicate that eastern part formed an outer fresh-water rim dominated by carbonate precipitation, grading westward into a saline lake with abundant precipitation of evaporites (Arenas and Pardo, 1999; Pardo et al., 2004) (Fig. 11D). Sediment supply of Pyrenean source outpacing accommodation determined a long-term (>20Myr) trend of southwards and then westward migration of the lacustrine environments (Anadon et al., 1989; Valero et al., 2014). Youngest preserved sedimentary units are currently attached towards the southern margin (Fig. 11E) and consist of palustrine to lacustrine limestone formations of latest Middle Miocene age (Pérez-Rivarés et al., 2018). These are the only remnants of this age, as their correlative soft and weakly consolidated alluvial sediments sourced from the Pyrenees were eroded after opening of the basin drainage.

In the shorter-term (10^4-10^6kyr), the alluvial-lacustrine units alternated to form cycles of expansion and retreat of the central lake. Cyclostratigraphic analysis of well dated sequences found these cycles to be orbitally controlled (Barberà et al., 1996; Luzón et al., 2002; Valero et al., 2014). Orbital eccentricity is seen as the pacemaker of short to long-term lacustrine sequences, and reveals a correlation of times of eccentricity maxima with periods of lake expansion, as found in lacustrine sequence of adjacent basins (Abdul Aziz et al., 2004; H. a. Abels et al., 2009; Hemmo a. Abels et al., 2009). The established correlation with Milankovitch frequencies suggests that (climatic) base level-driven lacustrine sequences were decoupled from (tectonic) supply-driven clastic sequences,

and that the sediment transfer systems of the Ebro was efficient to buffer the upstream tectonic signal for frequencies as low as the corresponding to the 2.4Myr eccentricity cycle. It is worth noting that low-gradient of the Ebro basin floor helped amplifying the effect of lake-level oscillations on the advances and retreats of the shoreline, a determinant factor in the distribution of sedimentary facies and the building of sedimentary sequences.

6. Final remarks

Tectonic growth and exhumation coupled with flexural subsidence are first-order controls on long-term sedimentation in foreland systems. Added on these, the regional paleogeographic context is a key to understand sedimentary trends and the location through time of sediment sinks. Very rapid filling of the Ripoll basin during the Early-Middle Eocene was favoured by its restricted connection with ocean basin. In contrast, the extended length and progressive compartmentalization of the sediment transfer system along the central and western Pyrenees favoured sediment accumulation in upstream areas, while open ocean connection to the west allowed sediment bypass. This resulted in a prolonged period, from Paleocene to late Eocene, of infill of the Jaca-Pamplona foredeep. Shifting into an internal drainage triggered rapid sediment aggradation, burial and stabilization of the frontal wedge, and then, reactivation of the uplift of the Axial zone (Beaumont et al., 2000; Costa et al., 2010). Here, timing was the key to find causal relationships, as the significant increase of sedimentation preceded the fast exhumation of the Axial Zone. Besides, it is likely that global cooling starting at the Eocene/Oligocene transition helped maintaining high-rates of erosion and sediment supply during the Oligocene (Parsons et al., 2012).

Drainage opening of the Ebro basin towards the Mediterranean was not a catastrophic event caused by the lake overspill. Capture of the internal drainage occurred gradually by fluvial piracy of a juvenile mountain river. Upstream incision until capture of the base level of the internal lake could last several millions of years until the base level of the interior lake was captured at an age younger than 11Ma, the age of the youngest preserved endorheic sedimentation. .

Steady long-term sedimentation rates are the general picture of the filling history of the SPFB, as a response to the long wave-length evolution of regional subsidence-driven accommodation. These

651 trends were only rarely interrupted, when a critical re-organization of the tectonic, climatic and
652 paleogeographic conditions took place. Long periods, lasting typically several million years, of
653 steady sedimentation predominate between punctuated episodes of reorganisation of the
654 sedimentary system.

655

656 **Acknowledgements**

657 This is a contribution of the research project CGL2014-55900-P, funded by MINECO (Spain).
658 Some of the authors are members of the consolidated research group of Geodynamics and Basin
659 Analysis 2017SGR596 of the Generalitat de Catalunya.
660

7. Figure captions

Figure 1. A geologic map of the NE Iberian Plate and the major Cenozoic structural units. Encircled red labels indicate magnetostratigraphic sections represented in Fig. 4. Thrusts sheet units: BC: Bóixols-Cotiella; MPM: Montsec-Peña Montañesa; GSM: Gavarnie-Serres Marginals; P: Pedraforca; CM: Cadí-Montgrí.

Figure 2. A chronostratigraphic panel along the eastern Ebro basin from the Pyrenees to the Catalan Coastal Ranges and the Linking Zone (Anadon et al., 1989; Anadón et al., 1979b; Barberà et al., 2001; Barnolas, 1992; Burbank et al., 1992; Busquets et al., 1992; Costa et al., 2010; Gómez-Paccard et al., 2012; Puigdefàbregas et al., 1986; Serra-Kiel et al., 2003b, 2003a; Vergés et al., 1998).

Figure 3. A chronostratigraphic panel of the Tremp-Graus, Ainsa and Jaca-Pamplona subbasins (Astibia et al., 2016; Barnolas and Gil-Pena, 2002; Beamud et al., 2011, 2003a; Bentham et al., 1992; Costa et al., 2013; Hogan and Burbank, 1996; López-Blanco et al., 2003; Mochales et al., 2012; Muñoz et al., 2013; Nijman, 1998; Oliva-Urcia et al., 2015; Oms et al., 2003; Payros et al., 2007; Puigdefàbregas, 1975; Rodríguez-Pintó et al., 2012; Roigé et al., 2017; Serra-Kiel et al., 1994; Vinyoles et al., 2019). Emplacement of thrusts: N: Nogueres, R: Rialp, O: Orri, M-PM: Montsec-Peña Montañesa, MP: Monte Perdido, G-SM: Gavarnie-Serres Marginals, G-SE: Gavarnie-Sierras Exteriores, Mo: Morreres.

Lithostratigraphic units: An, Antist; Gs, Graus; Co, Collegats; Se, Senterada; Ep, Espills; Pe, Pessonada; Gb, Gurb; Pl, Pallaresa; Er, Ermita; Cj-Cr, Cajigar-Cornudella; Si, Sis; Mr, Merli reef; Is/Be: Iscles-Berganuy reefs; Es, Escanilla; Bu, Buil; So, Sobrarbe; Gu, Guara; Gr, Grustán; Pa, Pano; Cp, Capella; Pr, Perarrúa; Cm, Campanué; Cst, Castissent; SM, Santa Marina, Cg, Castilgaleu; Ro, Roda; Po, Porredó; Su, Suerri Yb, Yeba; Ri, Riguala; Te, Tendrui; Me, Metils; Mi, Millaris; Al, Alveolina limestone. SV1-2: diferent units making the San Vicente Formation. PñO, Peña Oroel; SJP: San Juan de la Peña; Ca: Canciás; Sta.O: Santa Orosia; Li sdst.: Liédena sandstone

688 **Horizons:** EK, Ekzaba; UR, Urrotz; SÑ, Sabiñánigo; O, Olsón; EL, Escanilla limestone; SB, Santa
689 Bárbara; SP, San Pedro; SL, San Lino; M, Morillo limestone; A, Ascaso; LP, La Puebla; Lu, Santa
690 Llucia. 1 to 8 and a to g are different carbonate megaturbidite beds.

691 **Figure 4.** Magnetochronostratigraphic framework of the Paleogene and Neogene South-Pyrenean
692 Foreland basin infill. References to local magnetostratigraphic sections are as follows: 1) (Almar
693 et al., 2008); 2) (Juan C. Larrasoaña et al., 2006); 3) (Oliva-Urcia et al., 2019, 2015); 4) (Pérez-
694 Rivarés et al., 2018);5) (Pérez-Rivarés et al., 2004, 2002); 6) (Barberà et al., 2001; Valero et al.,
695 2014);7) (Jones et al., 2004); 8) (Costa et al., 2013, 2010); 9) (Gómez-Paccard et al., 2012); 10)
696 (Burbank et al., 1992; Vergès et al., 1998); 11) (Beamud et al., 2011, 2003b); 12) (Bentham and
697 Burbank, 1996; Mochales et al., 2012); 13) (Hogan and Burbank, 1996; Oms et al., 2003); 14)
698 (Costa et al., 2010; Hogan and Burbank, 1996; Rodríguez-Pintó et al., 2012). Note the different
699 graphic scale on the side of each magnetostratigraphic section. Geological Time Scale from Ogg
700 et al., (2016). The geographic location of sections is shown in Fig. 1.

701 **Figure 5.** A) A compilation of magnetozone's thicknesses as a function of the duration of their
702 respective chrons. Constant values of sedimentation rate are represented with diagonals in the plot.
703 The overall data from the SPFB yields sedimentation rates that range over two orders of magnitude,
704 between 0.05 and 1.0 m/kyr. However, taken each section individually, this variability is reduced
705 to within one order of magnitude. Note that the amplitude of these variations is not dependent on
706 the time window of measure (=chron duration), thus indicating that high amplitude variations
707 associated to the natural episodic behavior of sedimentation in clastic systems is buffered at the
708 time resolution of magnetostratigraphy. Each color represent a section, and the numbers indicate
709 sections from Figs 1 and 2. B) The amplitude of variation of the short-term sedimentation rate is
710 illustrated by calculating the rate of change between adjacent magnetozones. The histogram
711 indicates that the change of sedimentation rate is lower than a factor 2 for 80% of the data. This
712 contrasts with the relative duration of adjacent chrons of the Geological Time Scale, which is
713 higher than a factor of 2 for 60% of the data. These results show that the chaotic behavior of the
714 geomagnetic field has indeed resulted in a reversal pattern that is much more variable than the
715 averaged sedimentation rates and, therefore, that a good match of a magnetostratigraphic section
716 with the GPTS is a strong indication of a correct correlation.

Figure 6. Composite magnetostratigraphy and sedimentary trends of the Ripoll basin. Data collected from the Baga, Gombren and Sant Jaume de Frontanyà sections (Burbank et al., 1992; Vergés et al., 1998), and correlation revised according the new calibrated ages of shallow benthic foraminifera zone SBZ13 (Rodríguez-Pintó et al., 2012).

Figure 7. Composite stratigraphy and sedimentary trends of the Jaca-Pamplona basin. Data compiled from a Jaca composite section (Hogan and Burbank, 1996; Oms et al., 2003; Payros et al., 1999a), and Ara river section in Boltaña (Mochales et al., 2012).

Figure 8. Magnetostratigraphy and sedimentary trends in the southern margin of the Jaca basin (External Sierras). Data compiled from the Salinas, Arguis and Isuela sections (Costa et al., 2010; Hogan and Burbank, 1996; Kodama et al., 2010; Rodríguez-Pintó et al., 2012).

Figure 9. Magnetostratigraphy and sedimentary trends in the Eastern Ebro basin. Data compiled from the Miralles-La Tossa (Costa et al., 2013), Maians (Costa et al., 2010), and Rocafort, Sarral and Vinaixa (Barberà et al., 2001) sections.

Figure 10. Sedimentary trends during the Miocene in the central and western Ebro basin. Data compiled from the Albalatillo, Lanaja and San Caprasio (Pérez-Rivarés et al., 2002), Tarazona (Pérez-Rivarés et al., 2018), and Las Bardenas (Larrasoaña et al., 2006) sections.

Figure 11. Paleogeographic maps of the South Pyrenean Foreland basin. A) Paleocene; B) Early-Middle Eocene; C) Late Middle Eocene (Bartonian); D) Late Eocene-Oligocene; E) Middle-Late Miocene. Maps are constructed by considering displacement of thrust sheets relative to a fixed Iberian basement in its current coordinates. Data compiled from earlier studies (Anadon et al., 1989; Anadón et al., 1985; Arasa-Tuliesa and Cabrera, 2018; Beamud et al., 2003a; Beaumont et al., 2000; Carrigan et al., 2016; Carrillo, 2012; Costa et al., 2013, 2010; Jones et al., 2004; Lanaja et al., 1987; Larrasoaña et al., 2003; López-Blanco, 2002; Morsilli et al., 2012; Muñoz et al., 2013; Oliva-Urcia, 2018; Parcerisa et al., 2007; Pardo et al., 2004; Pérez-Rivarés et al., 2018; Popov et al., 2001; Puigdefàbregas, 1975; Pujadas et al., 1989; Pujalte et al., 2000; Roca, 1996; Roca et al., 1999; Tassone et al., 1994; Vergés, 2003, 1993; Villena et al., 1996) and authors' original data.

8. References

Ábalos, B., 2016. Geologic map of the Basque - Cantabrian Basin and a new tectonic interpretation of the Basque Arc. Int. J. Earth Sci. 105, 2327–2354. https://doi.org/10.1007/s00531-016-1291-6

Abdul Aziz, H., van Dam, J., Hilgen, F.J., Krijgsman, W., 2004. Astronomical forcing in Upper Miocene continental sequences: implications for the Geomagnetic Polarity Time Scale. Earth Planet. Sci. Lett. 222, 243–258. https://doi.org/10.1016/j.epsl.2004.02.018

Abels, Hemmo a., Abdul Aziz, H., Calvo, J.P., Tuenter, E., 2009. Shallow lacustrine carbonate microfacies document orbitally paced lake-level history in the Miocene Teruel Basin (North-East Spain). Sedimentology 56, 399–419. https://doi.org/10.1111/j.1365-3091.2008.00976.x

Abels, H. a., Aziz, H. a., Ventra, D., Hilgen, F.J., 2009. Orbital Climate Forcing in Mudflat to Marginal Lacustrine Deposits in the Miocene Teruel Basin (Northeast Spain). J. Sediment. Res. 79, 831–847. https://doi.org/10.2110/jsr.2009.081

Advokaat, E.L., Van Hinsbergen, D.J.J., Maffione, M., Langereis, C.G., Vissers, R.L.M., Cherchi, A., Schroeder, R., Madani, H., Columbu, S., 2014. Eocene rotation of Sardinia, and the paleogeography of the western Mediterranean region. Earth Planet. Sci. Lett. 401, 183–195. https://doi.org/10.1016/j.epsl.2014.06.012

Agustí, J., Pérez-Rivarés, F.J., Cabrera, L., Garcés, M., Pardo, G., Arenas, C., 2011. The Ramblian-Aragonian boundary and its significance for the European Neogene continental chronology. Contributions from the Ebro Basin record (NE Spain). Geobios 44, 121–134. https://doi.org/10.1016/j.geobios.2011.01.001

Alegret, L., Ortiz, S., Orue-Etxebarria, X., Bernaola, G., Baceta, J.I., Monechi, S., Apellaniz, E., Pujalte, V., 2009. the Paleocene-Eocene Thermal Maximum: New Data on Microfossil Turnover At the Zumaia Section, Spain. Palaios 24, 318–328. https://doi.org/10.2110/palo.2008.p08-057r

Allen, P.A., 2017. Sediment routing systems: The fate of sediment from source to sink. Cambridge

University Press.

Almar, Y., Garcés, M., Beamud, E., Muñoz, J.A., 2008. Timing and evolution of the structure of the southwestern Pyrenees from paleomagnetic analysis on its foreland basin (Ebro basin), in: VII Congreso Geológico de España 14-18 Julio. Las Palmas de Gran Canaria.

Anadon, P., Cabrera, L., Colldeforns, B., Sáez, A., 1989. Los sistemas lacustres del Eoceno superior y Oligoceno del sector oriental de la Cuenca del Ebro. Acta Geol. Hisp. 24, 205–230.

Anadón, P., Cabrera, L., Guimerà, J., Santanach, P., 1985. Paleogene strike-slip deformation and sedimentation along the southeastern margin of the Ebro Basin, in: Strike-Slip Deformation, Basin Formation, and Sedimentation. The Society of Economic Paleontologists and Mineralogists, pp. 303–318. https://doi.org/10.2110/pec.85.37.0303

Anadón, P., Colombo, F., Esteban, M., Marzo, M., Robles, S., Santanach, P., Solé Sugrañes, L., 1979a. Evolución tectonoestratigráfica de los Catalainides (*). Acta Geol. Hisp. 14, 242–270.

Anadón, P., Colombo, F., Esteban, M., Marzo, M., Robles, S., Santanach, P., Solé Sugrañes, L., 1979b. Evolución tectonoestratigráfica de los Catalainides. Acta Geol. Hisp. 14, 242–270.

Arasa-Tuliesa, A., Cabrera, L., 2018. Neogene-Quaternary onshore record in the lower Ebro river incised palaeovalley (Ebro margin, Catalan Coastal Range, NE Iberia). Geol. Acta 16, 265–292. https://doi.org/10.1344/GeologicaActa2018.16.3.3

Arche, A., Evans, G., Clavell, E., 2010. Some considerations on the initiation of the present SE Ebro River drainage system: Post- or pre-Messinian? J. Iber. Geol. 36, 73–85.

Arenas, C., Pardo, G., 1999. Latest Oligocene–Late Miocene lacustrine systems of the north-central part of the Ebro Basin (Spain): sedimentary facies model and palaeogeographic synthesis. Palaeogeogr. Palaeoclimatol. Palaeoecol. 151, 127–148. https://doi.org/10.1016/S0031-0182(99)00025-5

Astibia, H., Payros, A., Ortiz, S., Elorza, J., Álvarez-Pérez, G., Badiola, A., Bardet, N., Berreteaga,

A., Bitner, M.A., Calzada, S., Corral, J.C., Díaz-Martínez, I., Merle, D., Pacaud, J.M., Pereda-Suberbiola, X., Pisera, A., Rodríguez-Tovar, F.J., Tosquella, J., 2016. Fossil associations from the middle and upper eocene strata of the pamplona basin and surrounding areas (navarre, western pyrenees). J. Iber. Geol. 42, 7–28. https://doi.org/10.5209/rev_JIGE.2016.v42.n1.51601

Babault, J., Loget, N., Van Den Driessche, J., Castelltort, S., Bonnet, S., Davy, P., 2006. Did the Ebro basin connect to the Mediterranean before the Messinian salinity crisis? Geomorphology 81, 155–165. https://doi.org/10.1016/j.geomorph.2006.04.004

Badiola, A., Checa, L., Cuesta, M.A., Quer, R., Hooker, J.J., Astibia, H., 2009. The role of new Iberian finds in understanding European Eocene mammalian paleobiogeography. Geol. Acta 7, 243–258. https://doi.org/10.1344/105.000000281

Barberà, X., Cabrera, L., Marzo, M., Parés, J.M., Agustí, J., 2001. A complete terrestrial Oligocene magnetobiostratigraphy from the Ebro Basin, Spain. Earth Planet. Sci. Lett. 187, 1–16. https://doi.org/10.1016/S0012-821X(01)00270-9

Barberà, X., Cabrera, L., Marzo, M., Ripepe, M., 1996. Sedimentación lacustre y ciclicidad: las sucesiones fluvio-lacustres del Oligoceno superior del sector SE de la cuenca del Ebro. Geogaceta 20, 1072–1073.

Barnolas, A., 1992. Evolución sedimentaria de la Cuenca Surpirenaica Oriental durante el Eoceno. Acta Geol. Hisp. 27, 15–31.

Barnolas, A., Busquets, P., Serra-Kiel, J., 1981. Características sedimentológicas de la terminación del ciclo marino del Eoceno superior en el sector oriental de la Depresión del Ebro. Acta Geol. Hisp. 16, 215–221.

Barnolas, A., Gil-Pena, I., 2002. Ejemplos de relleno sedimentario multiepisodico en una cuenca de antepais fragmentada: La Cuenca Surpirenaica. Bol. Geol. y Min. 112, 17–38.

Beamud, E., Garcés, M., Cabrera, L., Muñoz, J.A., Almar, Y., 2003a. A new middle to late Eocene continental chronostratigraphy from NE Spain. Earth Planet. Sci. Lett. 216, 501–514.

https://doi.org/10.1016/S0012-821X(03)00539-9

Beamud, E., Garcés, M., Cabrera, L.L., Anton Munoz, J., Almar, Y., Muñoz, J.A., Almar, Y., Anton Muñoz, J., Anton Munoz, J., Almar, Y., 2003b. A new middle to late Eocene continental chronostratigraphy from NE Spain. Earth Planet. Sci. Lett. 216, 501–514. https://doi.org/10.1016/S0012-821X(03)00539-9

Beamud, E., Muñoz, J.A., Fitzgerald, P.G., Baldwin, S.L., Garcés, M., Cabrera, L., Metcalf, J.R., 2011. Magnetostratigraphy and detrital apatite fission track thermochronology in syntectonic conglomerates: constraints on the exhumation of the South-Central Pyrenees. Basin Res. 23, 309–331. https://doi.org/10.1111/j.1365-2117.2010.00492.x

Beaumont, C., Fullsack, P., Hamilton, J., 1992. Erosional control of active compressional orogens, in: Thrust Tectonics. Springer Netherlands, Dordrecht, pp. 1–18. https://doi.org/10.1007/978-94-011-3066-0_1

Beaumont, C., Muñoz, J.A., Hamilton, J., Fullsack, P., 2000. Factors controlling the Alpine evolution of the central Pyrenees inferred from a comparison of observations and geodynamical models. J. Geophys. Res. Solid Earth 105, 8121–8145. https://doi.org/10.1029/1999JB900390

Bentham, P., Burbank, D., 1996. Chronology of Eocene foreland basin evolution along the western oblique margin of the South-Central Pyrenees, in: Friend, P.F., Dabrio, C. (Eds.), Tertiary Basins of Spain: The Stratigraphic Record of Crustal Kinematics. Cambridge University Press, pp. 144–152.

Bentham, P.A., Burbank, D.W., Puigdefabregàs, C., 1992. Temporal and spatial controls on the alluvial architecture of an axial drainage system: late Eocene Escanilla Formation, southern Pyrenean foreland basin, Spain. Basin Res. 4, 335–352.

Bonilla-Salomón, I., Minwer-Barakat, R., Vianey-Liaud, M., 2016. Middle Eocene Rodents from Sant Jaume de Frontanyà-1 (Eastern Pyrenees, Northern Spain) and biochronological implications. J. Vertebr. Paleontol. 4634. https://doi.org/10.1080/02724634.2016.1121149

847 Borne, V., Margerel, J.P., Ollivier-Pierre, M.F., 1991. L'evolution des paléoenvironments au
848 Paléogène dans l'Ouest de la France. La bassin de Saffré-Nort-sur-Erdre (Loire-Atlantique,
849 France). Bull. Soc. Géol. Fr. 162, 739–751.

850 Burbank, D.W., Puigdefàbregas, C., Muñoz, J.A., 1992. The chronology of the Eocene tectonic
851 and stratigraphic development of the eastern Pyrenean foreland basin, northeast Spain. Geol.
852 Soc. Am. Bull. 104, 1101–1120. https://doi.org/10.1130/0016-7606(1992)104

853 Burbank, D.W., Vergés, J., 2004. Reconstruction of topography and related depositional systems
854 during active thrusting. J. Geophys. Res. Solid Earth 99, 20281–20297.
855 https://doi.org/10.1029/94jb00463

856 Busquets, P., Ramos Guerrero, E., Moya, S., Agusti, J., Colombo, F., Checa, L., Kohler, M., 1992.
857 La Formacion de Bellmunt (Unidad del Cadi, Pirineo Oriental); aportaciones
858 bioestratigraficas de los sistemas lacustres y palustres asociados. Acta Geol. Hisp. 27, 109–
859 116.

860 Caja, M.A., Permanyer, A., 2008. Significance of organic matter in eocene turbidite sediments (SE
861 Pyrenees, Spain). Naturwissenschaften 95, 1073–1077. https://doi.org/10.1007/s00114-008-
862 0416-6

863 Caja, M.A., Permanyer, A., Marfil, R., Al-Aasm, I.S., Martín-Crespo, T., 2006. Fluid flow record
864 from fracture-fill calcite in the Eocene limestones from the South-Pyrenean Basin (NE Spain)
865 and its relationship to oil shows. J. Geochemical Explor. 89, 27–32.
866 https://doi.org/10.1016/j.gexplo.2005.11.009

867 Cámara, P., Klimowitz, J., 2010. Interpretación geodinámica de la vertiente centro-occidental
868 surpirenaica (cuencas de Jaca-Tremp). Estud. Geológicos 41, 391.
869 https://doi.org/10.3989/egeol.85415-6720

870 Cantalejo, B., Pickering, K.T., 2014. Climate forcing of fine-grained deep-marine systems in an
871 active tectonic setting: Middle Eocene, Ainsa Basin, Spanish Pyrenees. Palaeogeogr.
872 Palaeoclimatol. Palaeoecol. 410, 351–371. https://doi.org/10.1016/j.palaeo.2014.06.005

873 Canudo, J.I., Molina, E., Rivellene, J., Serra−Kiel, J., Sucunza, M., 1988. Les événements
874 biostratigraphiques de la zone prépyrénéene d'Aragón (Espagne), de l'Eocene moyen a
875 l'Oligocène inférieure. Rev. Micropaleontol. 31, 15–29.

876 Carrigan, J.H., Anastasio, D.J., Kodama, K.P., Par, J.M., 2016. Fault-related fold kinematics
877 recorded by terrestrial growth strata , Sant Llorenç de Morunys , Pyrenees Mountains , NE
878 Spain s b. J. Struct. Geol. 91, 161–176. https://doi.org/10.1016/j.jsg.2016.09.003

879 Carrillo, E., 2012. Les Evaporites de la Conca Sud-pirinenca Oriental (Cuisià superior–Lutecià):
880 Sedimentologia i Estructura The Evaporites of the Southeastern Pyrenean Basin. PhD Thesis,
881 Universitat de Barcelona.

882 Cascella, A., Dinarès-Turell, J., 2009. Integrated calcareous nannofossil biostratigraphy and
883 magnetostratigraphy from the uppermost marine Eocene deposits of the southeastern
884 Pyrenean foreland basin : evidences for marine Priabonian deposition. Geol. Acta 7, 281–
885 296. https://doi.org/10.1344/105.000000282

886 Castelltort, S., Honegger, L., Adatte, T., Clark, J.D., Puigdefàbregas, C., Spangenberg, J.E.,
887 Dykstra, M.L., Fildani, A., 2017. Detecting eustatic and tectonic signals with carbon isotopes
888 in deep-marine strata, Eocene Ainsa Basin, Spanish Pyrenees. Geology 45, 707–710.
889 https://doi.org/10.1130/G39068.1

890 Castelltort, S.S., Van Den Driessche, J., 2003. How plausible are high-frequency sediment supply-
891 driven cycles in the stratigraphic record? Sediment. Geol. 157, 3–13.
892 https://doi.org/10.1016/S0037-0738(03)00066-6

893 Caus, E., 1973. Bioestratigrafía y Micropaleontología del Eoceno medio y superior del Prepirineo
894 catalán. Universitat Autònoma de Barcelona.

895 Chevrot, S., Sylvander, M., Diaz, J., Martin, R., Mouthereau, F., Manatschal, G., Masini, E.,
896 Calassou, S., Grimaud, F., Pauchet, H., Ruiz, M., 2018. The non-cylindrical crustal
897 architecture of the Pyrenees. Sci. Rep. 8, 9591. https://doi.org/10.1038/s41598-018-27889-x

898 Choukroune, P., 1989. The Ecors Pyrenean deep seismic profile reflection data and the overall

structure of an orogenic belt. Tectonics 8, 23–39. https://doi.org/10.1029/TC008i001p00023

Coney, P.J., Muñoz, J.A., McClay, K.R., Evenchick, C.A., 1996. Syntectonic burial and post-tectonic exhumation of the southern Pyrenees foreland fold–thrust belt. J. Geol. Soc. London. 153, 9–16. https://doi.org/10.1144/gsjgs.153.1.0009

Costa, E., Garcés, M., López-Blanco, M., Beamud, E., Gómez-Paccard, M., Larrasoaña, J.C., 2010. Closing and continentalization of the South Pyrenean foreland basin (NE Spain): magnetochronological constraints. Basin Res. 22, 904–917. https://doi.org/10.1111/j.1365-2117.2009.00452.x

Costa, E., Garcés, M., López-Blanco, M., Serra-Kiel, J., Bernaola, G., Cabrera, L.L., Beamud, E., 2013. The Bartonian-Priabonian marine record of the eastern south Pyrenean foreland basin (NE Spain): A new calibration of the larger foraminifers and calcareous nannofossil biozonation. Geol. Acta 11, 177–193. https://doi.org/10.1344/105.000001779

Cuenca Bescós, G., Canudo Sanagustín, J.I., Laplana Conesa, C., Moreno, J.A.A., 1992. Bio y cronoestratigrafía con mamíferos en la cuenca terciaria del Ebro: ensayo de síntesis. Acta Geol. Hisp. 27, 127–144.

Cuevas, J.L., 1992. Estratigrafía del “Garumniense” de la Conca de Tremp. Prepirineo de Lérida. Acta Geológica Hispánica 27, 95–108.

DeCelles, P.G., 2012. Foreland basin systems revisited: Variations in response to tectonic settings, in: Busby, C., Azor-Pérez, A. (Eds.), Tectonics of Sedimentary Basins: Recent Advances. Blackwell Publishing Ltd, pp. 405–426.

DeCelles, P.G., Giles, K., 1996. Foreland basin systems. Basin Res. 8, 105–123.

Evans, G., Arche, A., 2008. The flux of siliciclastic sediment from the Iberian Peninsula, with particular reference to the Ebro. Geol. Soc. London, Spec. Publ. 191, 199–208. https://doi.org/10.1144/gsl.sp.2002.191.01.14

Ferrer, J., 1971. El Paleoceno y Eoceno del borde suroriental de la Depresion del Ebro(Cataluna).

Mem. suisses del Paleontol. 90, 1–70.

Fitzgerald, P.G., Muñoz, J.A., Coney, P.J., Baldwin, S.L., 1999. Asymmetric exhumation across the Pyrenean orogen: Implications for the tectonic evolution of a collisional orogen. Earth Planet. Sci. Lett. 173, 157–170. https://doi.org/10.1016/S0012-821X(99)00225-3

Garcés, M., Agustí, J., Cabrera, L., Parés, J.M., 1996. Magnetostratigraphy of the Vallesian (late Miocene) in the Vallès-Penedès Basin (northeast Spain). Earth Planet. Sci. Lett. 142, 381–396.

Garcia-Castellanos, D., 2007. The role of climate during high plateau formation. Insights from numerical experiments. Earth Planet. Sci. Lett. 257, 372–390. https://doi.org/10.1016/j.epsl.2007.02.039

Garcia-Castellanos, D., Larrasoaña, J.C., 2015. Quantifying the post-tectonic topographic evolution of closed basins: The Ebro basin (northeast Iberia). Geology 43, 1–4. https://doi.org/10.1130/G36673.1

García-Senz, J., 2002. Cuencas Extensivas del Cretácico Inferior en los Pirineos Centrales, Formación y Subsecuente Inversión. PhD Thesis University of Barcelona.

García-Senz, J., Zamorano, M., 1992. Evolución tectónica y sedimentaria durante el Priaboniense superior-Mioceno inferior, en el frente de cabalgamiento de las Sierras Marginales occidentales. Acta Geol. Hisp. 27, 195–209.

Gómez-Paccard, M., López-Blanco, M., Costa, E., Garcés, M., Beamud, E., Larrasoaña, J.C.C., 2012. Tectonic and climatic controls on the sequential arrangement of an alluvial fan/fan-delta complex (Montserrat, Eocene, Ebro Basin, NE Spain). Basin Res. 24, 437–455. https://doi.org/10.1111/j.1365-2117.2011.00532.x

Grool, A.R., Ford, M., Vergés, J., Huismans, R.S., Christophoul, F., Dielforder, A., 2018. Insights Into the Crustal-Scale Dynamics of a Doubly Vergent Orogen From a Quantitative Analysis of Its Forelands: A Case Study of the Eastern Pyrenees. Tectonics 37, 450–476. https://doi.org/10.1002/2017TC004731

Hogan, P., Burbank, D., 1996. Evolution of the Jaca piggyback basin and emergence of the External Sierra, southern Pyrenees, in: Friend, P.F., Dabrio, C. (Eds.), Tertiary Basins of Spain: The Stratigraphic Record of Crustal Kinematics. Cambridge University Press, pp. 153–160.

Hottinger, L., 1960. Recherches sur les Alvéolines du Paléocène et de l'Eocène. PhD Thesis, Verlag nicht ermittelbar.

Huyghe, D., Castelltort, S., Mouthereau, F., Serra-Kiel, J., Filleaudeau, P.-Y., Emmanuel, L., Berthier, B., Renard, M., 2012. Large scale facies change in the middle Eocene South-Pyrenean foreland basin: The role of tectonics and prelude to Cenozoic ice-ages. Sediment. Geol. 253–254, 25–46. https://doi.org/10.1016/j.sedgeo.2012.01.004

ITGE, 1990. Documentos sobre la Geología del subsuelo de España. Vol. VI: Ebro-Pirineos.

Johnson, N.M., McGee, V.E., 1983. Magnetic polarity stratigraphy: Stochastic properties of data, sampling problems, and the evaluation of interpretations. J. Geophys. Res. 88, 1213–1221.

Jones, M. a., Heller, P.L., Roca, E., Garcés, M., Cabrera, L., 2004. Time lag of syntectonic sedimentation across an alluvial basin: theory and example from the Ebro Basin, Spain. Basin Res. 16, 489–506. https://doi.org/10.1111/j.1365-2117.2004.00244.x

Juez-Larré, J., Andriessen, P.A.M., 2002. Post Late Paleozoic tectonism in the southern Catalan Coastal Ranges (NE Spain), assessed by apatite fission track analysis. Tectonophysics 349, 113–129. https://doi.org/10.1016/S0040-1951(02)00049-5

Kendall, J., Vergés, J., Koshnaw, R., Louterbach, M., 2019. Petroleum tectonic comparison of fold and thrust belts: the Zagros of Iraq and Iran, the Pyrenees of Spain, the Sevier of Western USA and the Beni Sub-Andean of Bolivia. Geol. Soc. London, Spec. Publ. SP490-2018–102. https://doi.org/10.1144/SP490-2018-102

Kodama, K.P., Anastasio, D.J., Newton, M.L., Pares, J.M., Hinnov, L. a., 2010. High-resolution rock magnetic cyclostratigraphy in an Eocene flysch, Spanish Pyrenees. Geochemistry, Geophys. Geosystems 11, 1–22. https://doi.org/10.1029/2010GC003069

Labaume, P., Meresse, F., Jolivet, M., Teixell, A., Lahfid, A., 2016. Tectonothermal history of an exhumed thrust-sheet-top basin: An example from the south Pyrenean thrust belt. Tectonics 35, 1280–1313. https://doi.org/10.1002/2016TC004192

Labaume, P., Teixell, A., 2018. 3D structure of subsurface thrusts in the eastern Jaca Basin , southern Pyrenees. Geol. Acta 16, 477–498. https://doi.org/10.1344/GeologicaActa2018.16.4.9

Lanaja, J., Navarro, A., Martínez Abad, J., Del Valle, J., Ríos, L., Plaza, J., del Potro, R., Rodríguez de Pedro, J., 1987. Contribución de la exploración petrolifera al conocimiento de la Geología de España. Instituto Geológico y Minero de España.

Larrasoaña, Juan C., Murelaga, X., Garcés, M., 2006. Magnetobiochronology of Lower Miocene (Ramblian) continental sediments from the Tudela Formation (western Ebro basin, Spain). Earth Planet. Sci. Lett. 243, 409–423. https://doi.org/10.1016/j.epsl.2006.01.034

Larrasoaña, Juan C, Murelaga, X., Garcés, M., 2006. Magnetobiochronology of Lower Miocene (Ramblian) continental sediments from the Tudela Formation (western Ebro basin, Spain). Earth Planet. Sci. Lett. 243, 409–423. https://doi.org/10.1016/j.epsl.2006.01.034

Larrasoaña, J.C., Parés, J.M., Millán, H., Del Valle, J., Pueyo, E., 2003. Paleomagnetic , structural , and stratigraphic constraints on transverse fault kinematics during basin inversion : The Pamplona Fault (Pyrenees , north Spain). Tectonics 22. https://doi.org/10.1029/2002TC001446

Lawton, T.F., Roca, E., Guimerà, J., 1999. Kinematic-stratigraphic evolution of a growth syncline and its implications for tectonic development of the proximal foreland basin, southeastern Ebro basin, Catalunya, Spain. Bull. Geol. Soc. Am. 111, 412–431. https://doi.org/10.1130/0016-7606(1999)111<0412:KSEOAG>2.3.CO;2

Lewis, C.J., Vergés, J., Marzo, M., 2000. High mountains in a zone of extended crust: Insights into the Neogene-Quaternary topographic development of northeastern Iberia. Tectonics 19, 86–102. https://doi.org/10.1029/1999TC900056

López-Blanco, M., 2002. Sedimentary response to thrusting and fold growing on the SE margin of the Ebro basin (Paleogene, NE Spain). Sediment. Geol. 146, 133–154. https://doi.org/10.1016/S0037-0738(01)00170-1

López-Blanco, M., Marzo, M., Muñoz, J., 2003. Low-amplitude, synsedimentary folding of a deltaic complex: Roda Sandstone (lower Eocene), South-Pyrenean Foreland Basin. Basin Res.

Luzón, A., Gonzalez, A., Muñoz, A., Sánchez-Valverde, B., 2002. Upper Oligocene-Lower Miocene shallowing-upward lacustrine sequences controlled by periodic and non-periodic processes (Ebro Basin , northeastern Spain). J. Paleolimnol. 28, 441–456. https://doi.org/10.1023/A:1021675227754

Methner, K., Mulch, A., Fibieg, J., Wacker, U., Gerdes, A., Graham, S.A., Chamberlain, C.P., 2016. Rapid Middle Eocene temperature change in western North America. Earth Planet. Sci. Lett. 450, 132–139. https://doi.org/10.1016/j.epsl.2016.05.053

Michael, N.A., Carter, A., Whittaker, A.C., Allen, P.A., 2014. Erosion rates in the source region of an ancient sediment routing system: comparison of depositional volumes with thermochronometric estimates. J. Geol. Soc. London. 171, 401–412. https://doi.org/10.1144/jgs2013-108

Miller, K.G., Kominz, M.A., Browning, J. V., Wright, J.D., Mountain, G.S., Katz, M.E., Sugarman, P.J., Cramer, B.S., Christie-Blick, N., Pekar, S.F., 2005a. The Phanerozoic record of global sea-level change. Science 310, 1293–8. https://doi.org/10.1126/science.1116412

Miller, K.G., Wright, J.D., Browning, J. V., 2005b. Visions of ice sheets in a greenhouse world. Mar. Geol. 217, 215–231. https://doi.org/10.1016/j.margeo.2005.02.007

Mochales, T., Barnolas, a., Pueyo, E.L., Serra-Kiel, J., Casas, a. M., Samsó, J.M., Ramajo, J., Sanjuán, J., 2012. Chronostratigraphy of the boltaña anticline and the Ainsa Basin (southern pyrenees). Bull. Geol. Soc. Am. 124, 1229–1250. https://doi.org/10.1130/B30418.1

Molina, E., Alegret, L., Apellaniz, E., Bernaola, G., Caballero, F., Dinarès-turell, J., Hardenbol,

J., Heilmann-Clausen, C., Larrasoaña, J.C., Luterbacher, H., Monechi, S., Ortiz, S., Orue-Etxebarria, X., Payros, A., Pujalte, V., Rodríguez-Tovar, F.J., Tori, F., Tosquella, J., Uchman, A., 2011. The Global Stratotype Section and Point (GSSP) for the base of the Lutetian Stage at the Gorrondatxe section , Spain. Episodes 34, 86–108.

Molnar, P., England, P., 1990. Late Cenozoic uplift of mountain ranges and global climate change: chicken or egg? Nature 346, 29–34.

Morsilli, M., Bosellini, F.R., Pomar, L., Hallock, P., Aurell, M., Papazzoni, C.A., 2012. Mesophotic coral buildups in a prodelta setting (Late Eocene, southern Pyrenees, Spain): a mixed carbonate–siliciclastic system. Sedimentology 59, 766–794. https://doi.org/10.1111/j.1365-3091.2011.01275.x

Mouthereau, F., Filleaudeau, P.Y., Vacherat, A., Pik, R., Lacombe, O., Fellin, M.G., Castelltort, S., Christophoul, F., Masini, E., 2014. Placing limits to shortening evolution in the Pyrenees: Role of margin architecture and implications for the Iberia/Europe convergence. Tectonics 33, 2283–2314. https://doi.org/10.1002/2014TC003663

Mulch, A., Chamberlain, C.P., Cosca, M.A., Teyssier, C., Methner, K., Hren, M.T., Graham, S.A., 2015. Rapid change in high-elevation precipitation patterns of Western North America during the Middle Eocene Climatic Optimum (MECO). Am. J. Sci. https://doi.org/10.2475/04.2015.02

Muñoz-Jiménez, A., Casas-Sainz, A.M., 1997. The Rioja Trough (N Spain): tectosedimentary evolution of a symmetric foreland basin. Basin Res. 9, 65–85. https://doi.org/10.1046/j.1365-2117.1997.00031.x

Muñoz, J.-A.A., Beamud, E., Fernández, O., Arbués, P., Dinarès-Turell, J., Poblet, J., 2013. The Ainsa Fold and Thrust Oblique Zone of the Central Pyrenees: Kinematics of a Curved Contractional System from Paleomagnetic and Structural Data. Tectonics 32, 1142–1175. https://doi.org/10.1002/tect.20070

Muñoz, J.A., 2002. The pyrenees, in: Gibbons, W., Moreno, T. (Eds.), The Geology of Spain.

Geological Society London, pp. 370–385.

Muñoz, J.A., 1992. Evolution of a continental collision belt: ECORS-Pyrenees crustal balanced cross-section, in: McClay, K.R. (Ed.), Thrust Tectonics SE - 21. Springer Netherlands, pp. 235–246. https://doi.org/10.1007/978-94-011-3066-0_21

Muñoz, J.A., Mencós, J., Roca, E., Carrera, N., Gratacos, O., Ferrer, O., Fernández, O., 2018a. The structure of the South-Central Pyrenean fold and thrust belt as constrained by subsurface data. Geol. Acta 16, 439–460. https://doi.org/10.1344/GeologicaActa2018.16.4.7

Muñoz, J.A., Mencós, J., Roca, E., Carrera, N., Gratacós, O., Ferrer, O., Fernández, O., Gratacos, O., Ferrer, O., Fernández, O., 2018b. The structure of the South-Central Pyrenean fold and thrust belt as constrained by subsurface data. Geol. Acta 16, 439–460. https://doi.org/10.1344/GeologicaActa2018.16.4.7

Murelaga, X., Astibia, H., Sesé, C., Soria, M.D., Pereda Suberbiola, X., 2004. Mamíferos del Mioceno inferior de las Bardenas Reales de Navarra (Cuenca del Ebro, Península Ibérica). Munibe 55, 7–102.

Murelaga, X., Pérez-rivarés, F.J., Vázquez-Urbez, M., 2008. Nuevos datos bioestratigráficos y paleoecológicos del Mioceno medio (Aragoniense) del área de Tarazona de Aragón (Cuenca del Ebro , provincia de Zaragoza , España). Ameghiniana 45, 393–406.

Mutti, E., 1984. The Hecho Eocene submarine fan system, south-central Pyrenees, Spain. Geo-Marine Lett. 3, 199–202. https://doi.org/10.1007/BF02462468

Nijman, W., 1998. Cyclicity and basin axis shift in a piggyback basin: towards modelling of the Eocene Tremp-Ager Basin, South Pyrenees, Spain, Geological Society, London, Special Publications. https://doi.org/10.1144/GSL.SP.1998.134.01.07

Ogg, J.G., Ogg, G., Gradstein, F.M., 2016. A concise geologic time scale: 2016. Elsevier.

Oliva-Urcia, B., 2018. Thirty Years (1988-2018) of Advances in the Knowledge of the Structural Evolution of the South-Central Pyrenees During the Cenozoic Collision, a Summary. Rev. la

Soc. Geológica España 31, 51–68.

Oliva-Urcia, B., Beamud, E., Garcés, M., Abad, C.A., Ruth Soto, E.P., Pardo, G., 2015. New magnetostratigraphic dating of the Paleogene syntectonic sediments of the West-Central Pyrenees: Tectonostratigraphic implications, in: Geological Society of London, Special Publication.

Oliva-Urcia, B., Beamud, I., Arenas, C., Pueyo-Morer, E., Garcés, M., Soto, R., Valero, L., Pérez-Rivarés, F.J., 2019. Dating the northern deposits of the Ebro foreland basin; implications for the kinematics of the SW Pyrenean front. Tectonophysics in press. https://doi.org/10.1016/j.tecto.2019.05.007

Oms, O., Dinarès-Turell, J., Remacha, E., 2003. Magnetic stratigraphy from deep clastic turbidites: An example from the Eocene Hecho group (Southern Pyrenees). Stud. Geophys. Geod. 47, 275–288. https://doi.org/10.1023/A:1023719607521

Parcerisa, D., Roca, E., Madurell, J., Geologia, F. De, Barcelona, U. De, 2007. The Upper Oligocene of Montgat (Catalan Coastal Ranges, Spain): New age constrains to the western Mediterranean Basin opening. Geol. Acta 5, 3–17.

Pardo, G., Arenas, C., González, A., Luzón, A., Muñoz, A., Pérez, A., Pérez-Rivarés, F.J., Vázquez-Urbez, M., Villena, J., 2004. La cuenca del Ebro, in: Geología de España. SGE-IGME Madrid, pp. 533–543.

Parsons, A.J., Michael, N.A., Whittaker, A.C., Duller, R.A., Allen, P.A., 2012. Grain-size trends reveal the late orogenic tectonic and erosional history of the south-central Pyrenees, Spain. J. Geol. Soc. London. 169, 111–114. https://doi.org/10.1144/0016-76492011-087

Payros, A., Bernaola, G., Orue-Etxebarria, X., Dinarès-Turell, J., Tosquella, J., Apellaniz, E., 2007. Reassessment of the Early-Middle Eocene biomagnetochronology based on evidence from the Gorrondatxe section (Basque Country, western Pyrenees). Lethaia 40, 183–195. https://doi.org/10.1111/j.1502-3931.2007.00016.x

Payros, A., Martínez-Braceras, N., 2014. Orbital forcing in turbidite accumulation during the

Eocene greenhouse interval. Sedimentology 61, 1411–1432. https://doi.org/10.1111/sed.12113

Payros, A., Orue-Etxebarria, X., Pujalte, V., 2006. Covarying sedimentary and biotic fluctuations in Lower-Middle Eocene Pyrenean deep-sea deposits: Palaeoenvironmental implications. Palaeogeogr. Palaeoclimatol. Palaeoecol. 234, 258–276. https://doi.org/10.1016/j.palaeo.2005.10.013

Payros, A., Pujalte, V., Orue-etxebarria, X., 1999a. The South Pyrenean Eocene carbonate megabreccias revisited: New interpretation based on evidence from the Pamplona Basin. Sediment. Geol. 125, 165–194. https://doi.org/10.1016/S0037-0738(99)00004-4

Payros, A., Pujalte, V., Orue-Etxebarria, X., 1999b. The South Pyrenean Eocene carbonate megabreccias revisited: new interpretation based on evidence from the Pamplona Basin. Sediment. Geol. 125, 165–194. https://doi.org/10.1016/S0037-0738(99)00004-4

Payros, A., Tosquella, J., Bernaola, G., Dinarès-Turell, J., Orue-Etxebarria, X., Pujalte, V., 2009. Filling the North European Early/Middle Eocene (Ypresian/Lutetian) boundary gap: Insights from the Pyrenean continental to deep-marine record. Palaeogeogr. Palaeoclimatol. Palaeoecol. 280, 313–332. https://doi.org/10.1016/j.palaeo.2009.06.018

Pérez-Rivarés, F.J., Arenas, C., Pardo, G., Garcés, M., 2018. Temporal aspects of genetic stratigraphic units in continental sedimentary basins: Examples from the Ebro basin, Spain. Earth-Science Rev. 178, 136–153. https://doi.org/10.1016/j.earscirev.2018.01.019

Pérez-Rivarés, F.J., Garcés, M., Arenas, C., Pardo, G., 2004. Magnetostratigraphy of the Miocene continental deposits of the Montes de Castejón (central Ebro basin, Spain): Geochronological and paleoenvironmental implications. Geol. Acta 2, 221–234.

Pérez-Rivarés, J., Garcés, M., Arenas, C., Pardo, G., Pérez-Rivarés, F., 2002. Magnetocronología de la sucesión miocena de la Sierra de Alcubierre (Sector central de la Cuenca del Ebro). Rev. la Soc. Geológica España 15, 217–231.

Permanyer, A., Valles, D., 1988. Source Rock Potential of an Eocene Carbonate Slope: The

Armancies Formation of the South-Pyrenean Basin, Northeast Spain: ABSTRACT. Am. Assoc. Pet. Geol. Bull. 72, 25–28. https://doi.org/10.1306/703c967c-1707-11d7-8645000102c1865d

Pickering, K.T., Bayliss, N.J., 2009. Deconvolving tectono-climatic signals in deep-marine siliciclastics, Eocene Ainsa basin, Spanish Pyrenees: Seesaw tectonics versus eustasy. Geology 37, 203–206. https://doi.org/10.1130/G25261A.1

Pineda, A., 1996. El enlace y la paleogeografía neógena entre las cuencas del Duero y del Ebro en La Bureba (Burgos). Bol. Geol. y Min. 107, 14–28.

Plaziat, J., 1981. Late Cretaceous to late Eocene paleogeographic evolution of southwest Europe. Palaeogeogr. Palaeoclimatol. Palaeoecol. 36, 263–320.

Popov, S.., Akhmetiev, M.., Bugrova, E.., Lopatin, A. V, Amitrov, O.., Andreeva-Grigorovich, A.S., Zherikhin, V.., Zaporozhets, N.., Nikolaeva, I.., Krasheninnikov, V.., Kuzmicheva, E.., Sytchevskaya, E.., Shcherba, I.., 2001. Biogeography of the Northern Peri-Tethys from the Late Eocene to the Early Miocene: Part 1. Late Eocene. Paleontol. J. 35, S1–S68.

Puigdefàbregas, C., 1975. La sedimentación molásica de la Cuenca de Jaca. Pirineos 104, 188.

Puigdefàbregas, C., Muñoz, J.A., Marzo, M., 1986. Thrust Belt Development in the Eastern Pyrenees and Related Depositional Sequences in the Southern Foreland Basin, in: Allen, P.A., Homewood, P. (Eds.), Foreland Basins, Spec. Publs. Int. Ass. Sediment. 8. Blackwell Publishing Ltd., Oxford, UK, pp. 229–246. https://doi.org/10.1002/9781444303810.ch12

Pujadas, J., Casas, J.M., Muñoz, J., Sàbat, F., 1989. Thrust tectonics and Paleogene syntectonic sedimentation in the Empordà area (southeastern Pyrenees). Geodin. Acta 3, 195–206. https://doi.org/10.1080/09853111.1989.11105186

Pujalte, V., Baceta, J.I., Payros, A., 2002. Tertiary: Western Pyrenees and Basque-Cantabrian region, in: Gibbons, W., Moreno, T. (Eds.), The Geology of Spain. Geological Society of London, London. pp. 293–301.

Pujalte, V., Baceta, J.I., Payros, A., Orue-Etxebarria, X., Schmitz, B., 2000. Upper Paleocene—lower Eocene strata of the western Pyrenees, Spain: A shelf-to-basin correlation. GFF 122, 129–130.

Ramos, E., Busquets, P., Vergés, J., 2002. Interplay between longitudinal f luvial and transverse alluvial fan systems and growing thrusts in a piggyback basin (SE Pyrenees). Sediment. Geol. 146, 105–131.

Rego, E.S., Jovane, L., Hein, J.R., Sant'Anna, L.G., Giorgioni, M., Rodelli, D., Özcan, E., 2018. Mineralogical evidence for warm and dry climatic conditions in the Neo-Tethys (eastern Turkey) during the middle Eocene. Palaeogeogr. Palaeoclimatol. Palaeoecol. 501, 45–57. https://doi.org/10.1016/j.palaeo.2018.04.007

Remacha, E., Fernández, L.P., 2003. High-resolution correlation patterns in the turbidite systems of the Hecho Group (South-Central Pyrenees, Spain). Mar. Pet. Geol. 20, 711–726. https://doi.org/10.1016/j.marpetgeo.2003.09.003

Roca, E., 1996. La evolución geodinámica de la Cuenca Catalano-Balear y áreas adyacentes desde el Mesozoico hasta la actualidad. Acta Geol. Hisp. 29, 3–25.

Roca, E., Sans, M., Cabrera, L., Marzo, M., 1999. Oligocene to Middle Miocene evolution of the central Catalan margin (northwestern Mediterranean). Tectonophysics 315, 309–233.

Rodríguez-Pintó, a., Pueyo, E.L., Serra-Kiel, J., Samsó, J.M., Barnolas, a., Pocoví, a., 2012. Lutetian magnetostratigraphic calibration of larger foraminifera zonation (SBZ) in the Southern Pyrenees: The Isuela section. Palaeogeogr. Palaeoclimatol. Palaeoecol. 333–334, 107–120. https://doi.org/10.1016/j.palaeo.2012.03.012

Roigé, M., Gómez-Gras, D., Remacha, E., Boya, S., Viaplana-Muzas, M., Teixell, A., 2017. Recycling an uplifted early foreland basin fill: An example from the Jaca basin (Southern Pyrenees, Spain). Sediment. Geol. 360, 1–21. https://doi.org/10.1016/j.sedgeo.2017.08.007

Romans, B.W., Castelltort, S., Covault, J.A., Fildani, A., Walsh, J.P., 2016. Environmental signal propagation in sedimentary systems across timescales. Earth-Science Rev. 153, 7–29.

https://doi.org/10.1016/j.earscirev.2015.07.012

Salazar, A., 2003. El final del endorreismo terciario en la Cuenca del Ebro. Geotemas 5, 205–208.

Santolaria, P., Casas-Sainz, A.M., Soto, R., Casas, A., 2016. Gravity modelling to assess salt tectonics in the western end of the South Pyrenean Central Unit. J. Geol. Soc. London. 174, 269–288. https://doi.org/10.1144/jgs2016-027

Scotchman, J.I., Pickering, K.T., Sutcliffe, C., Dakin, N., Armstrong, E., 2015. Milankovitch cyclicity within the middle Eocene deep-marine Guaso System, Ainsa Basin, Spanish Pyrenees. Earth-Science Rev. 144, 107–121. https://doi.org/10.1016/j.earscirev.2015.01.007

Séguret, M., 1972. Étude tectonique des nappes et séries décollées de la partie centrale du versant sud des Pyrénées – Caractère synsédimentaire, rôle de la compression et de la gravité. Publications de l'Universite des Sciences et Techniques du Languedoc (USTELA), Montpellier, France.

Serra-Kiel, J., Canudo, J.I., Dinarès-Turell, J., Molina, E., Ortiz, N., Pascual, J., Samsó, J.M., Tosquella, J., 1994. Cronoestratigrafía de los sedimentos marinos del Terciario inferior de la Cuenca de Graus-Tremp (Zona Central Surpirenaica). Rev. la Soc. Geológica España 7, 273–297.

Serra-Kiel, J., Herrero, A.T. i, Palós, E.M. i, Briansó, E.S., Cañadell, C.F. i, Busquets, P. (Busquets i B., Angrill, J.T. i, Masip, J.V. i, 2003a. Marine and Transitional Middle/Upper Eocene Units of the Southeastern Pyrenean Foreland Basin (NE spain). Geol. Acta 1, 177–200. https://doi.org/10.1344/105.000001609

Serra-Kiel, J., Palós, E.M. i, Briansó, E.S., Cañadell, C.F. i, Pérez, G.Á., Busquets, P. (Busquets i B., Angrill, J.T. i, Faixa, J.F. i, Marsal, J.R., Barnolas, A., 2003b. An inventory of the Marine and Transitional Middle/Upper Eocene Deposits of the Southeastern Pyrenean Foreland Basin (NE spain). Geol. Acta 1, 201–232. https://doi.org/10.1344/105.000001610

Serra−Kiel, J., Hottinger, L., Caus, E., Drobne, K., Ferrandez-Canadell, C., Jauhri, A.K., Less, G., Pavlovec, R., Pignatti, J., Samsó, J.M., Schaub, H., Sirel, E., Strougo, A., Tambareau, Y.,

Tosquella, J., Zakrevskaya, E., 1998. Larger foraminiferal biostratigraphy of the Tethyan Paleocene and Eocene. Bull. Soc. Géol. Fr. 169, 281–299.

Sinclair, H.D., 1997. Tectonostratigraphic model for underfilled peripheral foreland basins: An Alpine perspective. Geol. Soc. Am. Bull. 109, 324–346. https://doi.org/10.1130/0016-7606(1997)109

Soto, R., Casas, A.M., Storti, F., Faccenna, C., 2002. Role of lateral thickness variations on the development of oblique structures at the Western end of the South Pyrenean Central Unit. Tectonophysics 350, 215–235. https://doi.org/10.1016/S0040-1951(02)00116-6

Struth, L., Garcia-Castellanos, D., Viaplana-Muzas, M., Vergés, J., 2019. Drainage network dynamics and knickpoint evolution in the Ebro and Duero basins: From endorheism to exorheism. Geomorphology 327, 554–571. https://doi.org/10.1016/J.GEOMORPH.2018.11.033

Tassone, A., Roca, E., Muñoz, J.A., Cabrera, L., Canals, M., 1994. Evolución del sector septentrional del margen continental catalán durante el Cenozoico. Acta Geológica Hispánica 29, 3–37.

Teixell, A., 1998. Crustal structure and orogenic material budget in the west central Pyrenees. Tectonics. https://doi.org/10.1029/98TC00561

Teixell, A., 1996. The Anso transect of the southern Pyrenees: basement and cover thrust geometries. J. Geol. Soc. London. 153, 301–310. https://doi.org/10.1144/gsjgs.153.2.0301

Thomson, K.D., Stockli, D.F., Clark, J.D., Puigdefàbregas, C., Fildani, A., 2017. Detrital zircon (U-Th)/(He-Pb) double-dating constraints on provenance and foreland basin evolution of the Ainsa Basin, south-central Pyrenees, Spain. Tectonics 36, 1352–1375. https://doi.org/10.1002/2017TC004504

Tosquella, J., Samsó, J.M., 1996. Bioestratigrafía y litoestratigrafia del paleoceno superior-eoceno inferior del sector oriental de la cuenca surpirenaica. Acta Geol. Hipanica 31, 3–21.

Urgeles, R., Camerlenghi, A., Garcia-Castellanos, D., De Mol B, Garces, M., Verges, J., Haslamk, I., Hardmank, M., De Mol, B., Garcés, M., Vergés, J., Haslam, I., Hardman, M., 2011. New constraints on the Messinian sealevel drawdown from3D seismic data of the Ebro Margin, western Mediterranean. Basin Res. 23, 123–145. https://doi.org/10.1111/j.1365-2117.2010.00477.x

Valero, L., Garcés, M., Cabrera, L., Costa, E., Sáez, L., 2014. 20 Myr of eccentricity paced lacustrine cycles in the Cenozoic Ebro Basin. Earth Planet. Sci. Lett. 408, 183–193.

van den Berg van Saparoea, A.P., Postma, G., Hampson, G.J., Steel, R.J., Burgess, P.M., Dalrymple, R.W., Others, 2008. Control of climate change on the yield of river systems. Recent Adv. Model. siliciclastic shallow-marine Stratigr.

Van Sickel, W.A., Kominz, M.A., Miller, K.G., Browning, J. V., 2004. Late Cretaceous and Cenozoic sea-level estimates: Backstripping analysis of borehole data, onshore New Jersey. Basin Res. 16, 451–465. https://doi.org/10.1111/j.1365-2117.2004.00242.x

Vergés, J., 2003. Evolución de los sistemas de rampas oblicuas de los Pirineos meridionales: fallas del Segre y Pamplona. Boletín Geológico y Min. 114, 87–101.

Vergés, J., 1993. Estudi geològic del vessant Sud del Pirineu Oriental i Central: Evolució en 3D. Universitat de Barcelona.

Vergés, J., Fernández, M., 2006. Ranges and basins in the Iberian Peninsula : their contribution to the present topography, in: Gee, D.G., Stephenson, R.A. (Eds.), Eurpean Lithospere Dynamics. Geological Society Memoirs, London. pp. 223–234.

Vergés, J., Fernàndez, M., Martìnez, A., Martínez, A., 2002. The Pyrenean orogen : pre- , syn- , and post-collisional evolution. J. Virtual Explor. 8, 55–74. https://doi.org/10.3809/jvirtex.2002.00058

Vergés, J., Marzo, M., Santaeulària, T., Serra-Kiel, J., Burbank, D.W., Muñoz, J.A., Giménez-Montsant, J., 1998. Quantified vertical motions and tectonic evolution of the SE Pyrenean foreland basin, in: Mascle, A., Puigdefàbregas, C., Luterbacher, H., Fernández, M. (Eds.),

Cenozoic Foreland Basins of Western Europe. Geological Society Special Publications, 134, pp. 107–134.

Vergés, J., Millán, H., Roca, E., Muñoz, J.A., Marzo, M., Cirés, J., Bezemer, T. Den, Zoetemeijer, R., Cloetingh, S., 1995. Eastern Pyrenees and related foreland basins: pre-, syn- and post-collisional crustal-scale cross-sections. Mar. Pet. Geol. 12, 903–915. https://doi.org/10.1016/0264-8172(95)98854-X

Vergés, J., Muñoz, J.A., 1990. Thrust sequence in the southern central Pyrenees. Bull. la Soc. Geol. Fr. VI, 265–271. https://doi.org/10.2113/gssgfbull.vi.2.265

Vergés, J., Muñoz, J.A., Martínez, A., 1992. South Pyrenean fold and thrust belt: The role of foreland evaporitic levels in thrust geometry, in: McClay, K.R. (Ed.), Thrust Tectonics SE - 23. Springer Netherlands, pp. 255–264. https://doi.org/10.1007/978-94-011-3066-0_23

Villena, J., Pardo, G., Pérez, A., 1996. E6 The Tertiary of the Iberian margin of the Ebro basin: paleogeography, in: Friend, P.F., Dabrio, C.J. (Eds.), Tertiary Basins of Spain: The Stratigraphic Record of Crustal Kinematics. Cambridge University Press, pp. 83–86.

Vincent, S.J., 2001. The Sis palaeovalley: A record of proximal fluvial sedimentation and drainage basin development in response to Pyrenean mountain building. Sedimentology 48, 1235–1276. https://doi.org/10.1046/j.1365-3091.2001.00421.x

Vinyoles, A., López-Blanco, M., Garcés, M., Arbués, P., Valero, L., Beamud, E., Oliva-Urcia, B., Cabello, P., 2019. 10 Myr evolution of sedimentation rates in a deep marine to non-marine foreland basin system: tectonic and sedimentary controls (Eocene, Tremp-Jaca basin, Southern Pyrenees, NE Spain). Basin Res. submitted.

Westerhold, T., Röhl, U., Donner, B., Frederichs, T., Kordesch, W.E.C., Bohaty, S.M., Hodell, D.A., Laskar, J., Zeebe, R.E., 2018. Late Lutetian Thermal Maximum—Crossing a Thermal Threshold in Earth's Climate System? Geochemistry, Geophys. Geosystems 19, 73–82. https://doi.org/10.1002/2017GC007240

Whitchurch, A.L., Carter, A., Sinclair, H.D., Duller, R.A., Whittaker, A.C., Allen, P.A., 2011.

Sediment routing system evolution within a diachronously uplifting orogen: Insights from detrital zircon thermochronological analyses from the South-Central Pyrenees. Am. J. Sci. 311, 442–482. https://doi.org/10.2475/05.2011.03

Zachos, J., Dickens, G., Zeebe, R., 2008. An early Cenozoic perspective on greenhouse warming and carbon-cycle dynamics. Nature 451, 279–283.

Zachos, J., Pagani, M., Sloan, L., Thomas, E., Billups, K., 2001. Trends, rhythms, and aberrations in global climate 65 Ma to present. Science (80-.). 292, 686–93. https://doi.org/10.1126/science.1059412

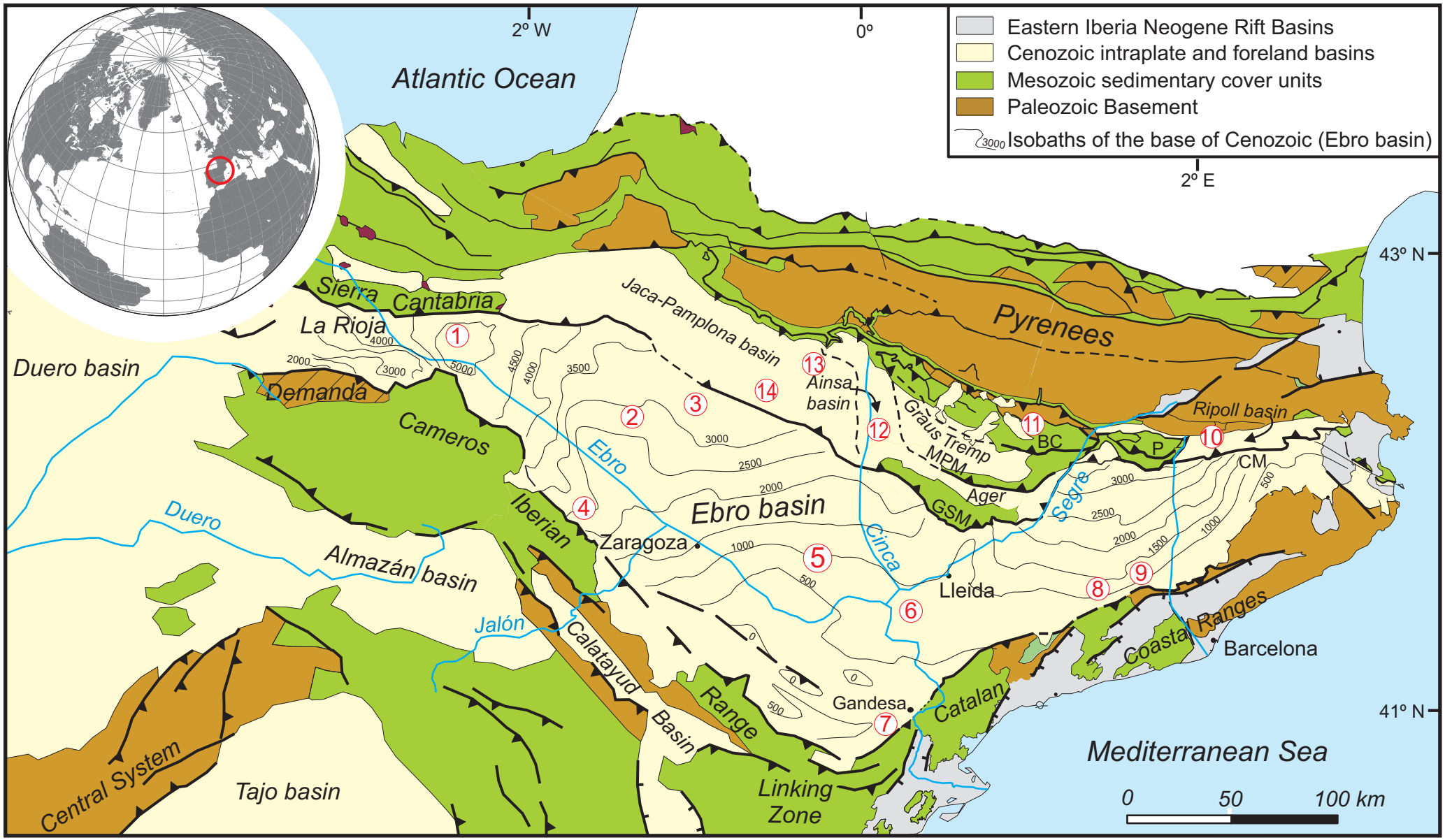
Eastern Iberia Neogene Rift Basins
Cenozoic intraplate and foreland basins
Mesozoic sedimentary cover units
Paleozoic Basement
3000 Isobaths of the base of Cenozoic (Ebro basin)
2º W
0º
2º E
43º N
41º N
Atlantic Ocean
Mediterranean Sea
Pyrenees
Sierra Cantabria
La Rioja
Jaca-Pamplona basin
Duero basin
Demanda
Cameros
Iberian
Ebro
Ebro basin
Ainsa basin
Graus Tremp
MPM
Ager
GSM
Segre
Cinca
Ripoll basin
BC
P
CM
Duero
Almazán basin
Jalón
Zaragoza
Lleida
Calatayud Basin
Range
Linking Zone
Catalan Coastal Ranges
Barcelona
Gandesa
Central System
Tajo basin
1
2
3
4
5
6
7
8
9
10
11
12
13
14
0
50
100 km

FIGURE 1

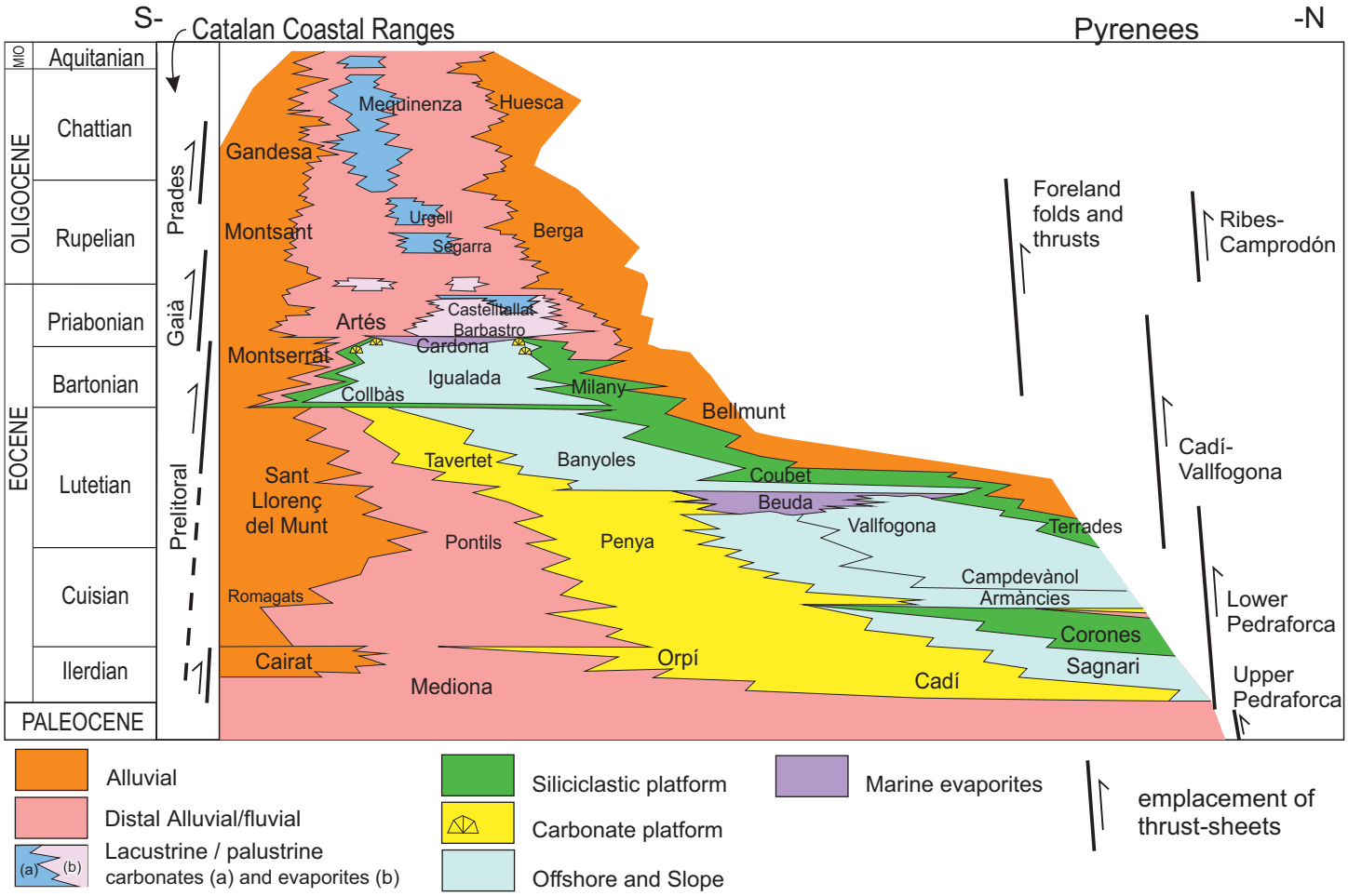
S-
Catalan Coastal Ranges
Pyrenees
-N
MIO
Aquitanian
OLIGOCENE
Chattian
Rupelian
EOCENE
Priabonian
Bartonian
Lutetian
Cuisian
Ilerdian
PALEOCENE
Prades
Gaià
Prelitoral
Meqdinenza
Huesca
Gandesa
Montsant
Urgell
Segarra
Berga
Artés
Castellfollat
Barbastro
Cardona
Montserrat
Igualada
Collbàs
Milany
Bellmunt
Tavertet
Banyoles
Coubet
Sant
Llorenç
del Munt
Beuda
Vallfogona
Terrades
Pontils
Penya
Campdevànol
Armàncies
Romagats
Corones
Sagnari
Cairat
Orpí
Cadí
Mediona
Foreland
folds and
thrusts
Ribes-
Camprodón
Cadí-
Vallfogona
Lower
Pedraforca
Upper
Pedraforca
Alluvial
Distal Alluvial/fluvial
Lacustrine / palustrine
carbonates (a) and evaporites (b)
(a)
(b)
Siliciclastic platform
Carbonate platform
Offshore and Slope
Marine evaporites
emplacement of
thrust-sheets

FIGURE 2

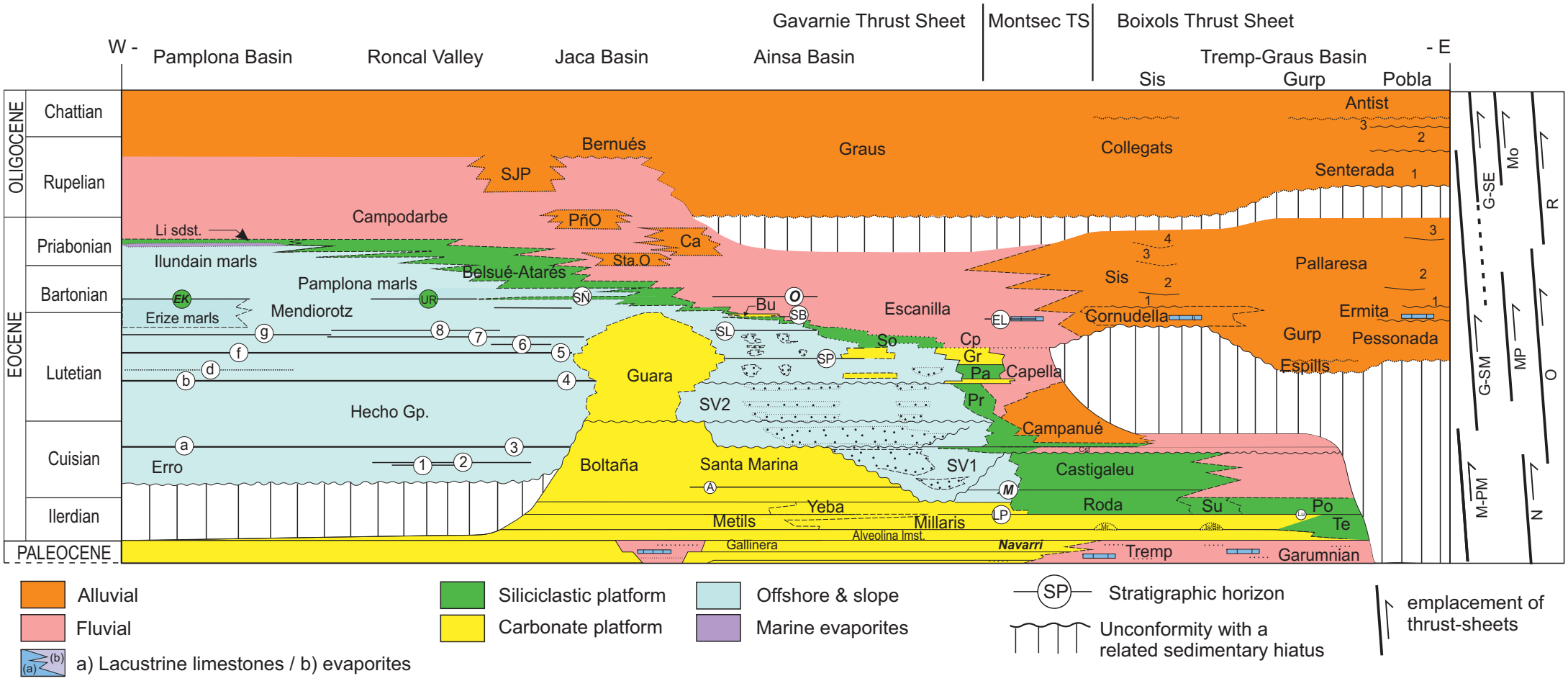
W -
Pamplona Basin
Roncal Valley
Jaca Basin
Ainsa Basin
Gavarnie Thrust Sheet
Montsec TS
Boixols Thrust Sheet
Tremp-Graus Basin
- E
Sis
Gurp
Pobla
OLIGOCENE
EOCENE
PALEOCENE
Chattian
Rupelian
Priabonian
Bartonian
Lutetian
Cuisian
Ilerdian
Bernués
SJP
Graus
Collegats
Antist
Senterada
Campodarbe
PñO
Ca
Sta.O
Li sdst.
Ilundain marls
Belsué-Atarés
Pamplona marls
Mendiorotz
Erize marls
Escanilla
Sis
Pallaresa
Cornudella
Ermita
Gurp
Pessonada
Espills
Guara
Hecho Gp.
SV2
Capella
Campanué
Erro
Boltaña
Santa Marina
SV1
Castigaleu
Roda
Su
Po
Te
Yeba
Metils
Millaris
Alveolina lmst.
Gallinera
Navarri
Tremp
Garumnian
G-SE
Mo
R
G-SM
MP
O
M-PM
N
Alluvial
Fluvial
a) Lacustrine limestones / b) evaporites
Siliciclastic platform
Carbonate platform
Offshore & slope
Marine evaporites
Stratigraphic horizon
Unconformity with a related sedimentary hiatus
emplacement of thrust-sheets

FIGURE 3

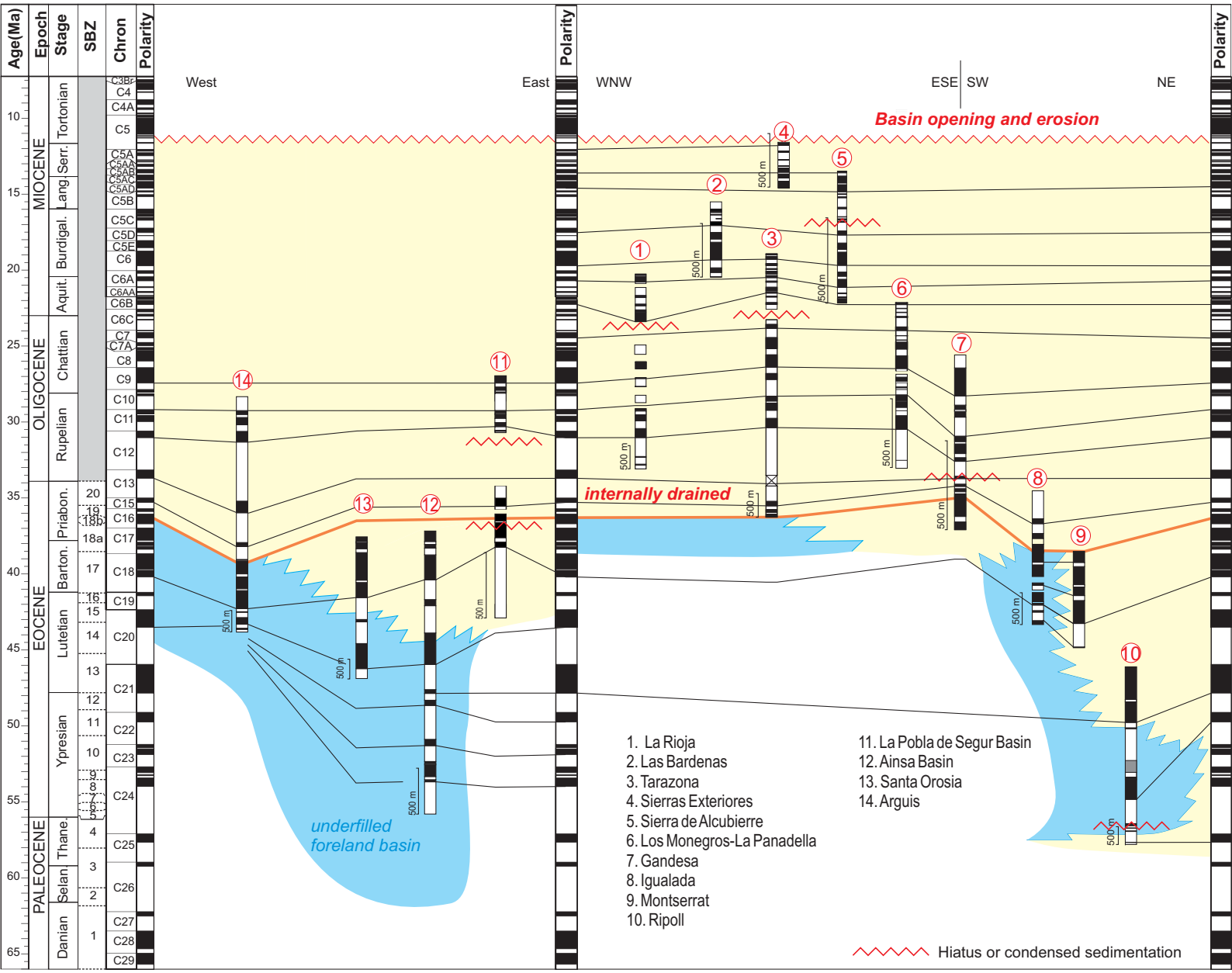
Age(Ma)
Epoch
Stage
SBZ
Chron
Polarity
West
East
WNW
ESE
SW
NE
Basin opening and erosion
internally drained
underfilled
foreland basin
500 m
1. La Rioja
2. Las Bardenas
3. Tarazona
4. Sierras Exteriores
5. Sierra de Alcubierre
6. Los Monegros-La Panadella
7. Gandesa
8. Igualada
9. Montserrat
10. Ripoll
11. La Pobla de Segur Basin
12. Ainsa Basin
13. Santa Orosia
14. Arguis
Hiatus or condensed sedimentation

FIGURE 4

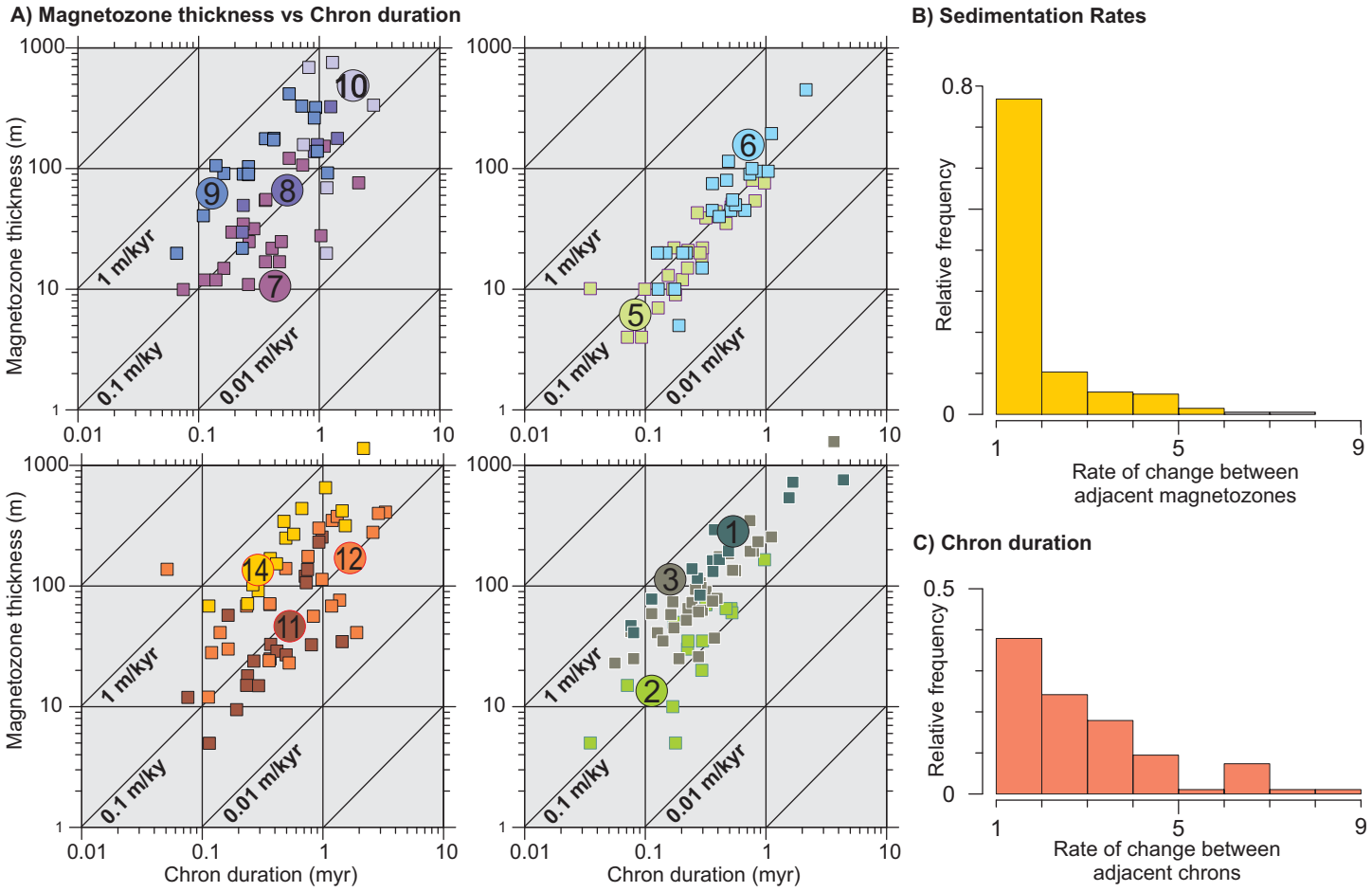
A) Magnetozone thickness vs Chron duration
B) Sedimentation Rates
C) Chron duration
Magnetozone thickness (m)
Chron duration (myr)
1 m/kyr
0.1 m/ky
0.01 m/kyr
Relative frequency
Rate of change between adjacent magnetozones
Rate of change between adjacent chrons

FIGURE 5

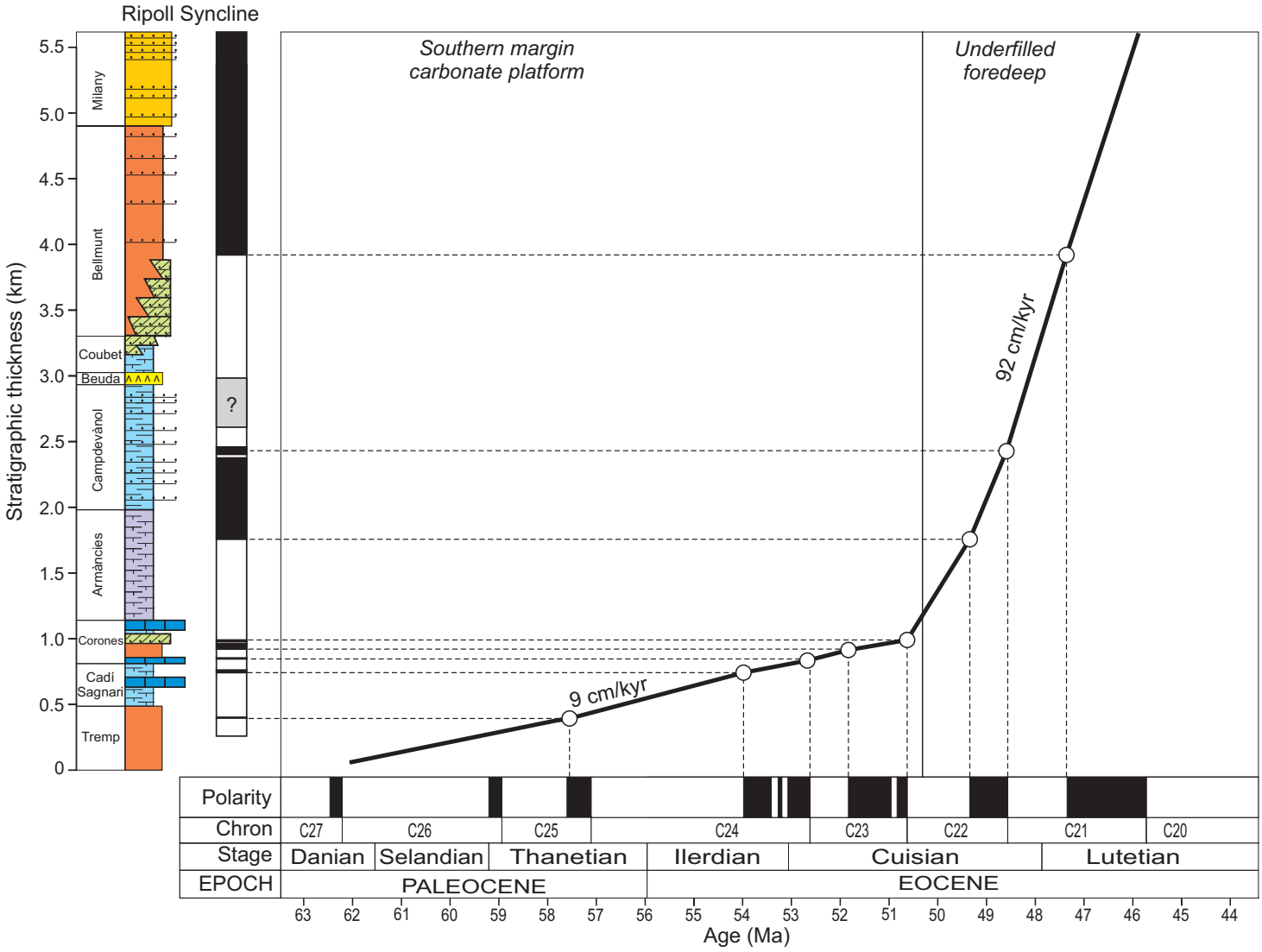
Ripoll Syncline
Stratigraphic thickness (km)
5.5
5.0
4.5
4.0
3.5
3.0
2.5
2.0
1.5
1.0
0.5
0
Milany
Bellmunt
Coubet
Beuda
Campdevànol
Armàncies
Corones
Cadí
Sagnari
Tremp
?
Southern margin
carbonate platform
Underfilled
foredeep
92 cm/kyr
9 cm/kyr
Polarity
Chron
C27
C26
C25
C24
C23
C22
C21
C20
Stage
Danian
Selandian
Thanetian
Ilerdian
Cuisian
Lutetian
EPOCH
PALEOCENE
EOCENE
63
62
61
60
59
58
57
56
55
54
53
52
51
50
49
48
47
46
45
44
Age (Ma)

FIGURE 6

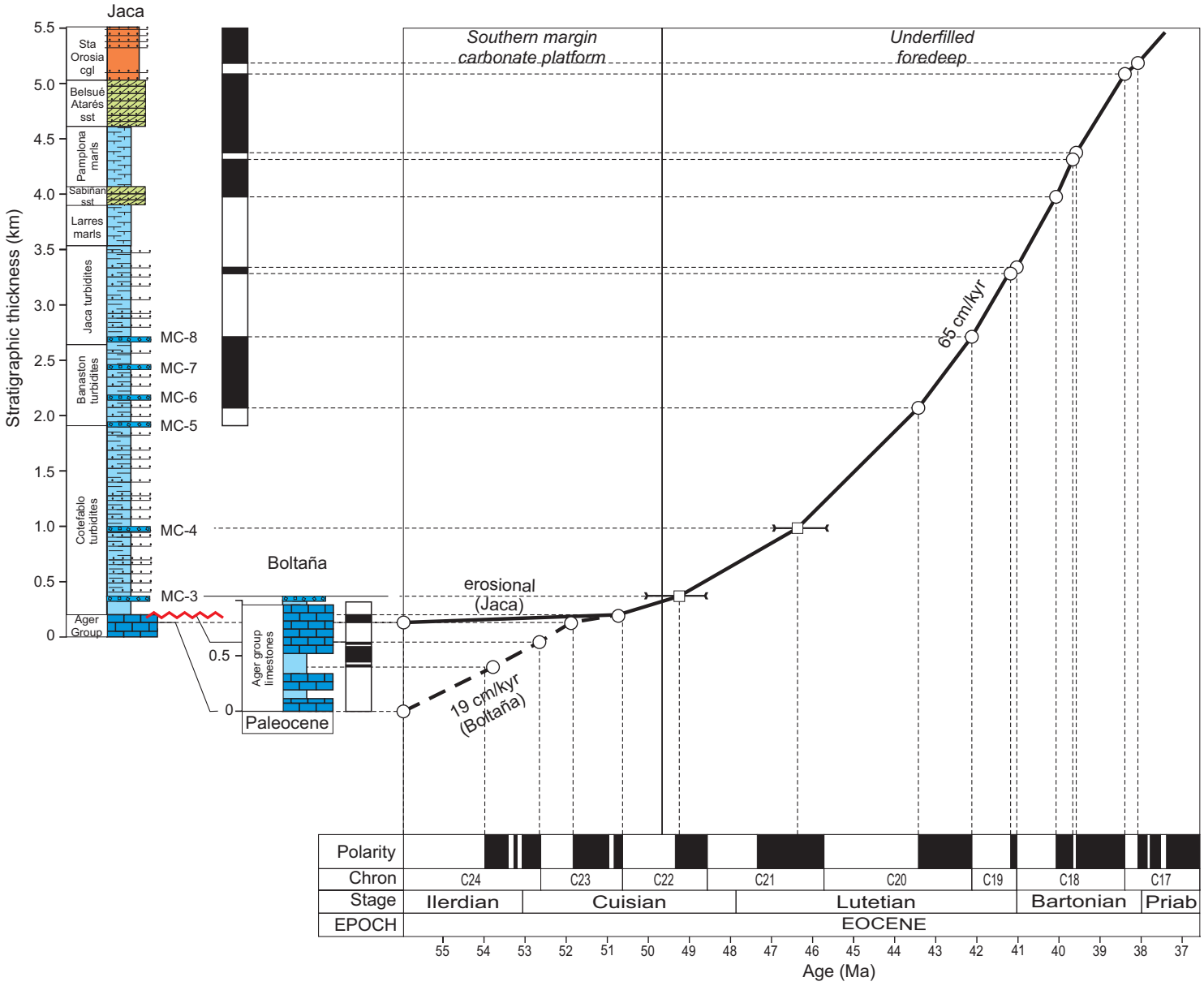
Jaca
Sta Orosia cgl
Belsué Atarés sst
Pamplona marls
Sabiñan sst
Larres marls
Jaca turbidites
Banaston turbidites
Cotefablo turbidites
Ager Group
MC-8
MC-7
MC-6
MC-5
MC-4
MC-3
Stratigraphic thickness (km)
5.5
5.0
4.5
4.0
3.5
3.0
2.5
2.0
1.5
1.0
0.5
0
Boltaña
Ager group limestones
0.5
0
Paleocene
Southern margin carbonate platform
Underfilled foredeep
erosional (Jaca)
65 cm/kyr
19 cm/kyr (Boltaña)
Polarity
Chron
C24
C23
C22
C21
C20
C19
C18
C17
Stage
Ilerdian
Cuisian
Lutetian
Bartonian
Priab
EPOCH
EOCENE
55
54
53
52
51
50
49
48
47
46
45
44
43
42
41
40
39
38
37
Age (Ma)

FIGURE 7

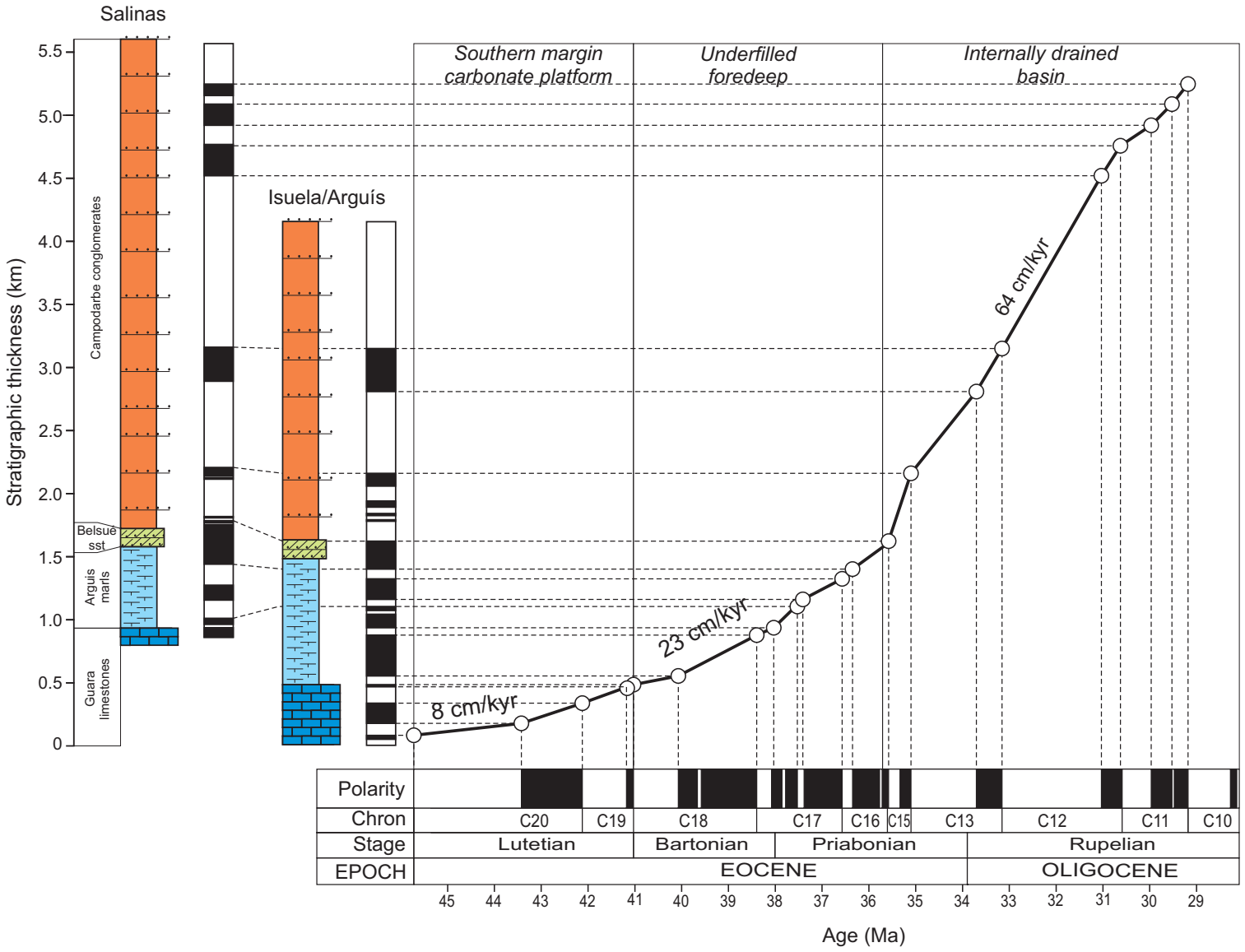
Salinas
Isuela/Arguís
Stratigraphic thickness (km)
5.5
5.0
4.5
4.0
3.5
3.0
2.5
2.0
1.5
1.0
0.5
0
Campodarbe conglomerates
Belsué sst
Arguis marls
Guara limestones
Southern margin carbonate platform
Underfilled foredeep
Internally drained basin
8 cm/kyr
23 cm/kyr
64 cm/kyr
Polarity
Chron
C20
C19
C18
C17
C16
C15
C13
C12
C11
C10
Stage
Lutetian
Bartonian
Priabonian
Rupelian
EPOCH
EOCENE
OLIGOCENE
45
44
43
42
41
40
39
38
37
36
35
34
33
32
31
30
29
Age (Ma)

FIGURE 8

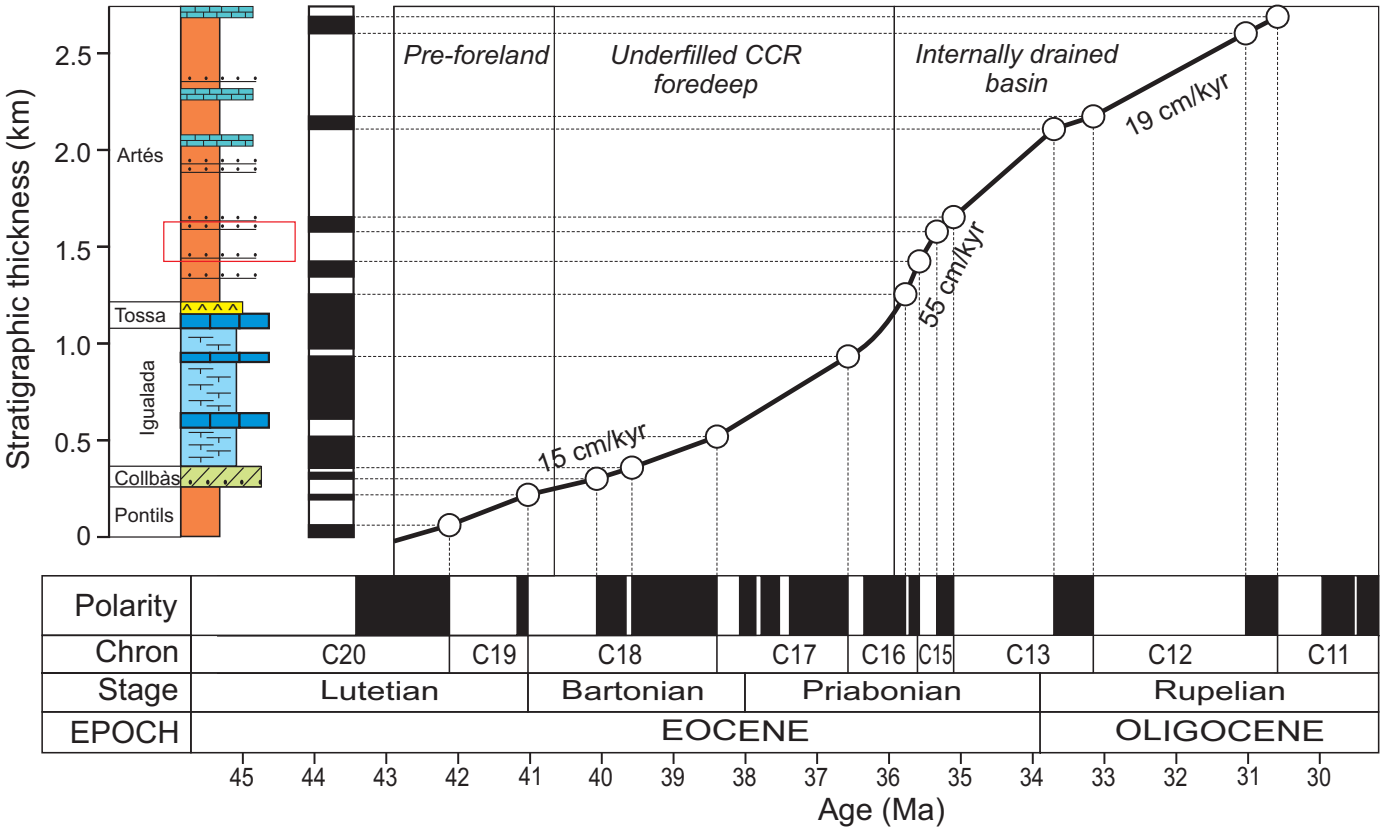
Stratigraphic thickness (km)
2.5
2.0
1.5
1.0
0.5
0
Artés
Tossa
Igualada
Collbàs
Pontils
Pre-foreland
Underfilled CCR foredeep
Internally drained basin
15 cm/kyr
55 cm/kyr
19 cm/kyr
Polarity
Chron
C20
C19
C18
C17
C16
C15
C13
C12
C11
Stage
Lutetian
Bartonian
Priabonian
Rupelian
EPOCH
EOCENE
OLIGOCENE
45
44
43
42
41
40
39
38
37
36
35
34
33
32
31
30
Age (Ma)

FIGURE 9

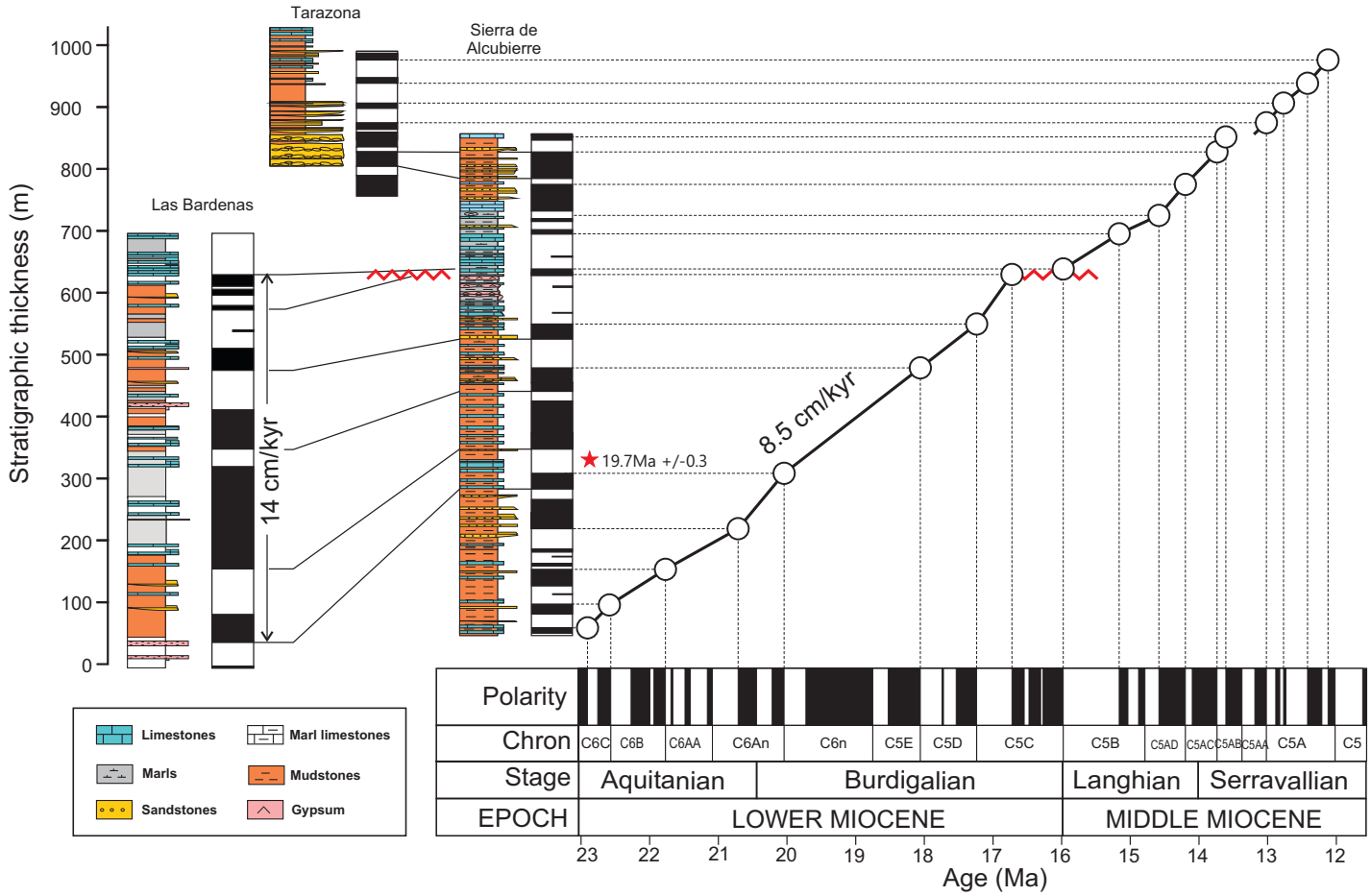
Tarazona
Sierra de Alcubierre
Las Bardenas
Stratigraphic thickness (m)
1000
900
800
700
600
500
400
300
200
100
0
14 cm/kyr
19.7Ma +/-0.3
8.5 cm/kyr
Limestones
Marl limestones
Marls
Mudstones
Sandstones
Gypsum
Polarity
Chron
C6C
C6B
C6AA
C6An
C6n
C5E
C5D
C5C
C5B
C5AD
C5AC
C5AB
C5AA
C5A
C5
Stage
Aquitanian
Burdigalian
Langhian
Serravallian
EPOCH
LOWER MIOCENE
MIDDLE MIOCENE
23
22
21
20
19
18
17
16
15
14
13
12
Age (Ma)

FIGURE 10

PALEOCENE (Thanetian)
~57Ma

Bay of Biscay

Itzurun

Barrica - Elgoibar

Azcoitia - Leiza

Lakora

Muñorodero - San Cibrián

Legumbe

Mondarruego - San Urbez
(Gallinera)

Bóixols

Montsec

Biure

Garumnian facies

Garumnian facies

N

Logroño

Huesca

Zaragoza

Lleida

Girona

Barcelona

Tarragona

Exposed

Alluvial conglomerates

Alluvial fines / fluvial

Offshore

Carbonate platform

Reverse fault

Anticline fold

0

200 km

FIGURE 11A

EOCENE (lower Lutetian)
~52 Ma

N

PYRENEES

Aralar-Bilbao

Roncesvalles

M. Perdido fold & thrust system

Orri uplift

Broto

Jaca basin

Lower Pedraforca

Figueres

Gavarnie S.M thrust system

Guara 1

Vallfogona

Ripoll basin

Beuda

Penya

Girona

Prelitoral thrust

CATALAN Coastal Ranges

La Salut

Pontils

Barcelona

Tarragona

SS

Logroño

Huesca

Zaragoza

Lleida

Exposed
Alluvial conglomerates
Alluvial fines / fluvial
Lacustrine
Coastal (detrital)
Offshore (t: turbidites)
Marine evaporites
Carbonate platform

Reverse fault
Anticline fold
non-active faults
water divide

0 200 km

FIGURE 11B

EOCENE (Bartonian-Priabonian)
~38Ma

N

Bilbao-Aralar
Pamplona
Roncesvalles
Millares + Guara-Gedre + Guarga uplift
Orri uplift
Freser Antiformal stack uplift
Vallfogona
Montgrí-Roc de Frausa
Gavarnie - Sm thrust system
Cameros-Demanda
Prelitoral
Catalan Coastal Ranges
water divide in the NPZ
Jaca basin
Ebro basin
Pamplona
Logroño
Huesca
Zaragoza
Lleida
Tarragona
Barcelona
Girona
Igualada
SS

Exposed
Alluvial conglomerates
Alluvial fines / fluvial
Coastal (detrital)
Offshore
Marine evaporites
Carbonate platform

Normal fault
Reverse fault
Flexure
Anticline fold
non-active faults
water divide

0 200 km

FIGURE 11C

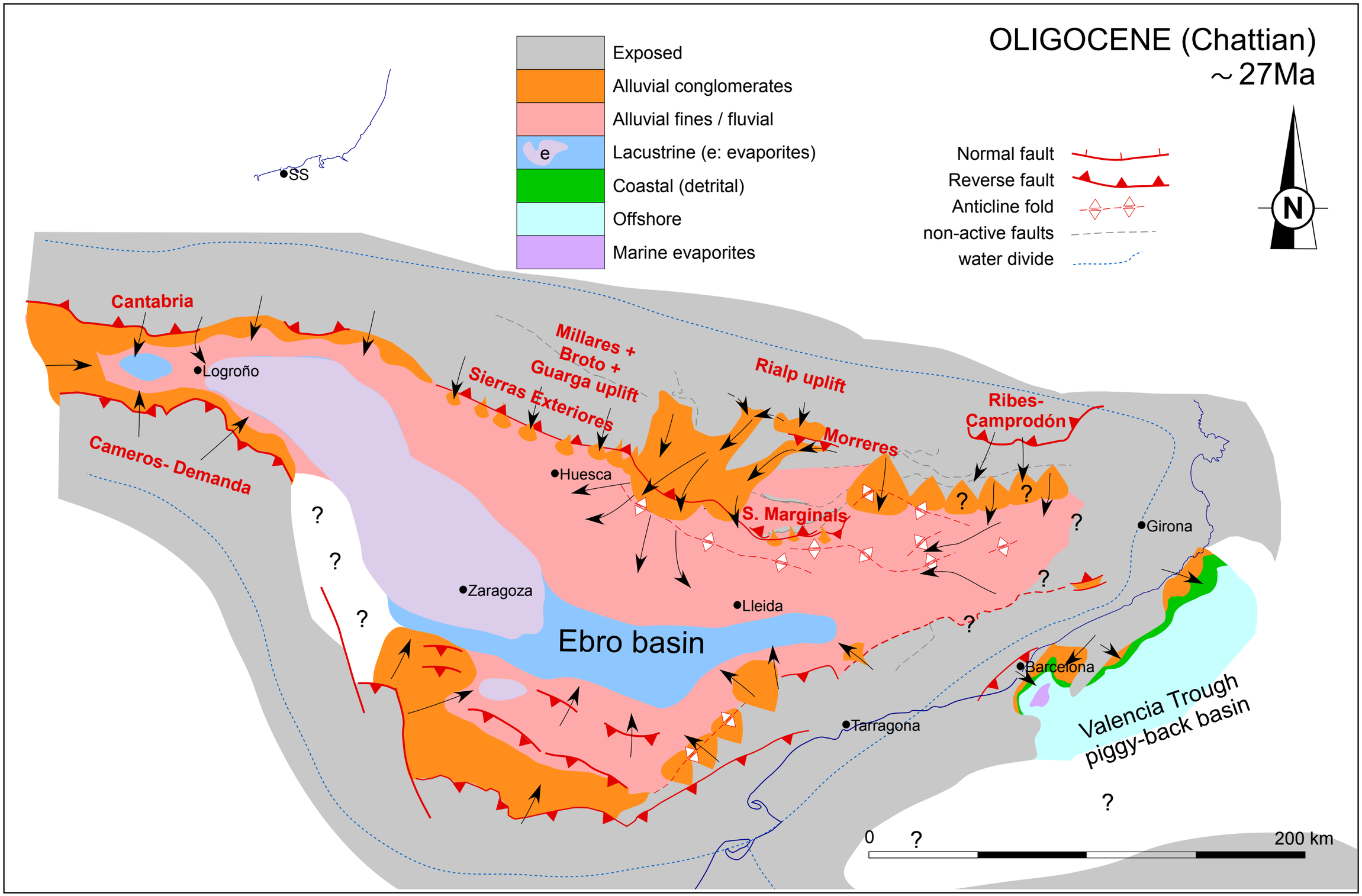
OLIGOCENE (Chattian)
~27Ma
Exposed
Alluvial conglomerates
Alluvial fines / fluvial
Lacustrine (e: evaporites)
Coastal (detrital)
Offshore
Marine evaporites
e
Normal fault
Reverse fault
Anticline fold
non-active faults
water divide
N
SS
Cantabria
Logroño
Cameros- Demanda
Millares +
Broto +
Guarga uplift
Sierras Exteriores
Rialp uplift
Morreres
Ribes-
Camprodón
Huesca
S. Marginals
Girona
Zaragoza
Lleida
Ebro basin
Barcelona
Tarragona
Valencia Trough
piggy-back basin
?
0
200 km

FIGURE 11D

MIOCENE (Serravallian-Tortonian)
~10Ma

N

SS

Cantabria

Pamplona

Logroño

Cameros-Demanda

?

Huesca

?

Zaragoza

Lleida

Ebro basin

?

?

?

?

La Cerdanya

Girona

Vallès-Penedès

Barcelona

Barcelona

El Camp

Tarragona

?

?

?

Exposed

Alluvial conglomerates

Alluvial fines / fluvial

Lacustrine

Coastal (detrital)

Offshore

Normal fault

Reverse fault

Anticline fold

non-active faults

water divide

0

200 km

FIGURE 11E